

ASSEA

N 68-18828

FACILITY FORM 602	(ACCESSION NUMBER)	(THRU)
	51	1
	(PAGES)	(CODE)
	CR - 93486	OES
	(NASA CR OR TMX OR AD NUMBER)	(CATEGORY)

GPO PRICE \$ \_\_\_\_\_

CSFTI PRICE(S) \$ \_\_\_\_\_

Hard copy (HC) 3.00

Microfiche (MF) .65

RESEARCH ON THE POLARIZATION IN POROUS OXYGEN  
ELECTRODES

Contract No. NASW - 1536

Third Quarterly Report

Period Covered: October 1, 1967 - December 31, 1967

Issued January 24, 1968

Prepared for

National Aeronautics and Space Administration

Washington, D.C.

Written by:

*Ingemar Lindholm*

Ingemar Lindholm  
Chemistry Laboratory

*Ingrid Edwardsson*

Ingrid Edwardsson  
Chemistry Laboratory

Approved by:

*Oto von Krusenstierna*

Oto von Krusenstierna  
Manager Chemistry Laboratory

*Olle Lindström*

Olle Lindström  
Director of Central Laboratories



ALLMÄNNA SVENSKA ELEKTRISKA AKTIEBOLAGET  
Chemistry Laboratory, Fuel Cell Research  
Västerås, Sweden.

## TABLE OF CONTENTS

	<u>Page</u>
ABSTRACT	III
LIST OF TABLES	IV
LIST OF FIGURES	V
1. SUMMARY	1
2. EXPERIMENTAL TECHNIQUE FOR ELECTRODE EVALUATION	2
2.1 Physical Measurements on Electrodes	2
2.2 Electrochemical Measurements on Electrodes	2
2.3 Electrode Preparation	4
3. EXPERIMENTAL RESULTS	5
3.1 Physical properties of electrodes with Ag, Pd and Pt electrocatalysts	5
3.2 Electrochemical comparison for electrodes with Ag, Pd and Pt electrocatalysts	6
3.3 The decay of polarization with time for Ag, Pd and Pt electrocatalysts	10
3.4 Pore structure	13
4. OXYGEN REDUCTION - DIFFERENT ELECTROCATALYSTS. DISCUSSION.	15
4.1 General	15
4.2 Reaction mechanism on carbon	15
4.3 Reaction mechanism on metals	16

## TABLE OF CONTENTS

	<u>Page</u>
ABSTRACT	III
LIST OF TABLES	IV
LIST OF FIGURES	V
1. SUMMARY	1
2. EXPERIMENTAL TECHNIQUE FOR ELECTRODE EVALUATION	2
2.1 Physical Measurements on Electrodes	2
2.2 Electrochemical Measurements on Electrodes	2
2.3 Electrode Preparation	4
3. EXPERIMENTAL RESULTS	5
3.1 Physical properties of electrodes with Ag, Pd and Pt electrocatalysts	5
3.2 Electrochemical comparison for electrodes with Ag, Pd and Pt electrocatalysts	6
3.3 The decay of polarization with time for Ag, Pd and Pt electrocatalysts	10
3.4 Pore structure	13
4. OXYGEN REDUCTION - DIFFERENT ELECTROCATALYSTS. DISCUSSION.	15
4.1 General	15
4.2 Reaction mechanism on carbon	15
4.3 Reaction mechanism on metals	16

	<u>Page</u>
4.5 Adsorption on the electrode surface	18
4.6 Open circuit potential	19
4.7 Comparison at high polarization	20
4.8 Comparison with mathematical treatment of the "Thin-film model"	21
5. CONCLUSIONS AND FUTURE PLANS	23
6. LIST OF REFERENCES	24

	<u>Page</u>
4.5 Adsorption on the electrode surface	18
4.6 Open circuit potential	19
4.7 Comparison at high polarization	20
4.8 Comparison with mathematical treatment of the "Thin-film model"	21
5. CONCLUSIONS AND FUTURE PLANS	23
6. LIST OF REFERENCES	24

## ABSTRACT

The objective of this investigation is to study mass transport polarization and activation polarization in porous oxygen electrodes.

The polarization in porous nickel electrodes has been measured with varying electrocatalysts, silver, palladium and platinum. The mass transport properties of the KOH electrolyte, e.g. oxygen solubility, oxygen diffusivity and ionic conductivity have been varied by changing the KOH-concentration from 1 M KOH to 10 M KOH at 50°C and the temperature from 25°C to 85°C with 7 M KOH.

The polarization decay with time after current interruption has been studied for Ag, Pd and Pt electrocatalysts.

## ABSTRACT

The objective of this investigation is to study mass transport polarization and activation polarization in porous oxygen electrodes.

The polarization in porous nickel electrodes has been measured with varying electrocatalysts, silver, palladium and platinum. The mass transport properties of the KOH electrolyte, e.g. oxygen solubility, oxygen diffusivity and ionic conductivity have been varied by changing the KOH-concentration from 1 M KOH to 10 M KOH at 50°C and the temperature from 25°C to 85°C with 7 M KOH.

The polarization decay with time after current interruption has been studied for Ag, Pd and Pt electrocatalysts.

## LIST OF TABLES

<u>Table</u>	<u>Page</u>
1. BET surface area and porosity for different active layers	5
2. b-values in mV for different electro-catalysts	8
3. Exchange current density in 7 M KOH A/cm <sup>2</sup> (electrode cross section surface)	9
4. Activation energy for oxygen reduction in 7 M KOH at -300 and - 500 mV vs reversible oxygen potential in same solution kcal/mole, temperature range 25 - 85°C	10
5. Kinetic and physical parameters	22

## LIST OF TABLES

<u>Table</u>	<u>Page</u>
1. BET surface area and porosity for different active layers	5
2. b-values in mV for different electro-catalysts	8
3. Exchange current density in 7 M KOH A/cm <sup>2</sup> (electrode cross section surface)	9
4. Activation energy for oxygen reduction in 7 M KOH at -300 and - 500 mV vs reversible oxygen potential in same solution kcal/mole, temperature range 25 - 85°C	10
5. Kinetic and physical parameters	22

## LIST OF FIGURES

<u>Figure</u>	<u>Page</u>
1. Current density vs differential pressure. Palladium electrocatalyst. 7 M KOH, 50° <sup>o</sup> C	27
2. Polarization curves at optimum differential pressure with varying electrolyte concentration. Palladium electrocatalyst	28
3. Polarization curves at optimum differential pressure for silver, palladium and platinum electrocatalysts compared with a nickel structure without catalyst. 25° <sup>o</sup> C, 7 M KOH	29
4. Polarization curves at optimum differential pressure for silver, palladium and platinum electrocatalysts compared with a nickel structure without catalyst. 70° <sup>o</sup> C, 7 M KOH	30
5. Comparison between the inverse slope of the polarization curve, $\frac{di}{d\eta}$ at a high polarization, and a mass transport function $\sqrt{S D_F}$ calculated for KOH electrolyte. Palladium electrocatalyst	31
6. Polarization curves at optimum differential pressure at varying temperature. Platinum electrocatalyst	32
7. Arrhenius plot for electrodes with different electrocatalysts at 300 and 500 mV polarization	33
8. Processes in a porous electrode before and after current interruption	34
9. Polarization decay for an electrode with silver electrocatalyst from 350 mV polarization. Varying differential pressure.	35

## LIST OF FIGURES

<u>Figure</u>	<u>Page</u>
1. Current density vs differential pressure. Palladium electrocatalyst. 7 M KOH, 50°C	27
2. Polarization curves at optimum differential pressure with varying electrolyte concentration. Palladium electrocatalyst	28
3. Polarization curves at optimum differential pressure for silver, palladium and platinum electrocatalysts compared with a nickel structure without catalyst. 25°C, 7 M KOH	29
4. Polarization curves at optimum differential pressure for silver, palladium and platinum electrocatalysts compared with a nickel structure without catalyst. 70°C, 7 M KOH	30
5. Comparison between the inverse slope of the polarization curve, $\frac{di}{d\eta}$ at a high polarization, and a mass transport function $\sqrt{S D_F}$ calculated for KOH electrolyte. Palladium electrocatalyst	31
6. Polarization curves at optimum differential pressure at varying temperature. Platinum electrocatalyst	32
7. Arrhenius plot for electrodes with different electrocatalysts at 300 and 500 mV polarization	33
8. Processes in a porous electrode before and after current interruption	34
9. Polarization decay for an electrode with silver electrocatalyst from 350 mV polarization. Varying differential pressure.	35

<u>Figure</u>	<u>Page</u>
10. Polarization decay for an electrode with silver electrocatalyst in 2 M KOH and 10 M KOH from 350 and 500 mV polarization	36
11. Polarization decay from 350 mV polarization, for silver, palladium and platinum electrocatalysts	37
12. Polarization decay from 350 mV polarization for an electrode with platinum electrocatalyst. Varying electrolyte temperature	38
13. Relative volume of solid, liquid and gas in the active layer as a function of the differential pressure. 7 M KOH, 50°C	39
14. Film area $\text{cm}^2/\text{cm}^2$ electrode cross section as a function of the differential pressure. 7 M KOH, 50°C	40
15. Film resistance as a function of differential pressure. 7 M KOH, 50°C	41
16. Relative film conductivity as a function of the amount of electrolyte in the pore system 7 M KOH, 50°C	42
17. Film conductivity, film area and current density as a function of differential pressure. Silver electrocatalyst, 7 M KOH, 50°C, increasing differential pressure	43
18. Comparison of the shape of our experimental curves with numerical calculations for the "Thin-film model"	44

<u>Figure</u>	<u>Page</u>
10. Polarization decay for an electrode with silver electrocatalyst in 2 M KOH and 10 M KOH from 350 and 500 mV polarization	36
11. Polarization decay from 350 mV polarization, for silver, palladium and platinum electrocatalysts	37
12. Polarization decay from 350 mV polarization for an electrode with platinum electrocatalyst. Varying electrolyte temperature	38
13. Relative volume of solid, liquid and gas in the active layer as a function of the differential pressure. 7 M KOH, 50°C	39
14. Film area $\text{cm}^2/\text{cm}^2$ electrode cross section as a function of the differential pressure. 7 M KOH, 50°C	40
15. Film resistance as a function of differential pressure. 7 M KOH, 50°C	41
16. Relative film conductivity as a function of the amount of electrolyte in the pore system 7 M KOH, 50°C	42
17. Film conductivity, film area and current density as a function of differential pressure. Silver electrocatalyst, 7 M KOH, 50°C, increasing differential pressure	43
18. Comparison of the shape of our experimental curves with numerical calculations for the "Thin-film model"	44

1

## SUMMARY

An experimental investigation of oxygen reduction in porous electrodes shows that the surface reaction is rate-limiting for Ag, Pd and Pt electrocatalysts in porous nickel electrodes at a low polarization from reversible oxygen electrode. This process has a higher activation energy, around 8 kcal/mole, than mass transport which is rate-limiting at a higher polarization for Ag, Pd and Pt electrocatalysts with a lower activation energy, around 5 kcal/mole.

Silver gives a lower polarization than palladium and platinum at low current densities, presumably due to a difference in electrosorption or faster decompositon of hydrogen peroxide ion ( $\text{HO}_2^-$ ) on silver.

The rate of oxygen reduction at high polarization is determined by mass transport and approximatively the same for all these electrocatalysts.

The shape of current density vs differential pressure ( $i - p$ ) curves at constant potential are the same for palladium and platinum as measured earlier for silver.

The shape of the polarization curves is in agreement with a numerical calculation with the "thin-film model" considering all forms of polarization.

Palladium and platinum give almost straight Tafel lines between 0,5 and 5 mA/cm<sup>2</sup> with a slope of 48 mV for Pd and 55 mV for Pt. The exchange current density is about  $10^{-10}$  A/cm<sup>2</sup> for Pt and smaller than  $10^{-11}$  A/cm<sup>2</sup> for Pd (real catalyst surface area) in 7 M KOH at 50°C.

1

## SUMMARY

An experimental investigation of oxygen reduction in porous electrodes shows that the surface reaction is rate-limiting for Ag, Pd and Pt electrocatalysts in porous nickel electrodes at a low polarization from reversible oxygen electrode. This process has a higher activation energy, around 8 kcal/mole, than mass transport which is rate-limiting at a higher polarization for Ag, Pd and Pt electrocatalysts with a lower activation energy, around 5 kcal/mole.

Silver gives a lower polarization than palladium and platinum at low current densities, presumably due to a difference in electrosorption or faster decompositon of hydrogen peroxide ion ( $\text{HO}_2^-$ ) on silver.

The rate of oxygen reduction at high polarization is determined by mass transport and approximatively the same for all these electrocatalysts.

The shape of current density vs differential pressure ( $i - p$ ) curves at constant potential are the same for palladium and platinum as measured earlier for silver.

The shape of the polarization curves is in agreement with a numerical calculation with the "thin-film model" considering all forms of polarization.

Palladium and platinum give almost straight Tafel lines between 0,5 and 5 mA/cm<sup>2</sup> with a slope of 48 mV for Pd and 55 mV for Pt. The exchange current density is about  $10^{-10}$  A/cm<sup>2</sup> for Pt and smaller than  $10^{-11}$  A/cm<sup>2</sup> for Pd (real catalyst surface area) in 7 M KOH at 50°C.

2

## EXPERIMENTAL TECHNIQUES FOR ELECTRODE EVALUATION

2.1

### Physical Measurements on Electrodes

The characterization and physical evaluation of electrodes generally involved the determination of surface and porosity. The methods were described in our First Quarterly Report (1).

As the electrocatalysts were sintered, spottests were made with an electron microsond to see if any alloys had been formed with the carrier material nickel. This microsond investigation was made by Dr G Carlsson at the Swedish Institute for Metal Research.

2.2

### Electrochemical Measurements on Electrodes

It is necessary to have a reference potential when the current density from the i-p and i-v curves are compared for varying electrolyte concentration and temperature. The reversible oxygen potential in the same solution is the most suitable reference potential. These electrodes are not reversible oxygen electrodes, and the reversible oxygen potential must be known from other information. The reversible oxygen potential for each combination of KOH-concentration and temperature was calculated with methods described in our First Quarterly Report.

Investigation of varying differential pressures with constant potential (i-p curves) and polarization curves (i-v curves) with constant pressure were made at varying temperature and electrolyte concentration. The measurements were done with porous electrodes of two layers: a coarse active layer of nickel with silver, palladium or platinum as an electrocatalyst and a fine porous layer of nickel facing the electrolyte side.

2

## EXPERIMENTAL TECHNIQUES FOR ELECTRODE EVALUATION

2.1

### Physical Measurements on Electrodes

The characterization and physical evaluation of electrodes generally involved the determination of surface and porosity. The methods were described in our First Quarterly Report (1).

As the electrocatalysts were sintered, spottests were made with an electron microsond to see if any alloys had been formed with the carrier material nickel. This microsond investigation was made by Dr G Carlsson at the Swedish Institute for Metal Research.

2.2

### Electrochemical Measurements on Electrodes

It is necessary to have a reference potential when the current density from the i-p and i-v curves are compared for varying electrolyte concentration and temperature. The reversible oxygen potential in the same solution is the most suitable reference potential. These electrodes are not reversible oxygen electrodes, and the reversible oxygen potential must be known from other information. The reversible oxygen potential for each combination of KOH-concentration and temperature was calculated with methods described in our First Quarterly Report.

Investigation of varying differential pressures with constant potential (i-p curves) and polarization curves (i-v curves) with constant pressure were made at varying temperature and electrolyte concentration. The measurements were done with porous electrodes of two layers: a coarse active layer of nickel with silver, palladium or platinum as an electrocatalyst and a fine porous layer of nickel facing the electrolyte side.

2

## EXPERIMENTAL TECHNIQUES FOR ELECTRODE EVALUATION

### 2.1

#### Physical Measurements on Electrodes

The characterization and physical evaluation of electrodes generally involved the determination of surface and porosity. The methods were described in our First Quarterly Report (1).

As the electrocatalysts were sintered, spottests were made with an electron microsond to see if any alloys had been formed with the carrier material nickel. This microsond investigation was made by Dr G Carlsson at the Swedish Institute for Metal Research.

### 2.2

#### Electrochemical Measurements on Electrodes

It is necessary to have a reference potential when the current density from the i-p and i-v curves are compared for varying electrolyte concentration and temperature. The reversible oxygen potential in the same solution is the most suitable reference potential. These electrodes are not reversible oxygen electrodes, and the reversible oxygen potential must be known from other information. The reversible oxygen potential for each combination of KOH-concentration and temperature was calculated with methods described in our First Quarterly Report.

Investigation of varying differential pressures with constant potential (i-p curves) and polarization curves (i-v curves) with constant pressure were made at varying temperature and electrolyte concentration. The measurements were done with porous electrodes of two layers: a coarse active layer of nickel with silver, palladium or platinum as an electrocatalyst and a fine porous layer of nickel facing the electrolyte side.

The electrocatalytic activity was measured in half-cells with  $\phi$  35 mm porous discs as oxygen electrodes in a holder. The potential is measured against a H<sub>2</sub> reference electrode and controlled by an ASEA potentiostat.

I-p curves were measured at a potential of -350 mV vs the reversible oxygen potential in the same solution with a differential pressure range of 0,2 - 1,4 atm. Polarization curves (i-v) were measured for each combination of electrolyte concentration and temperature, with an optimum differential pressure.

I-p and i-v curves are measured stepwise with an interval of 3 minutes. The selected potential of -350 mV gives a high reaction rate on the electrocatalyst but a low rate on the carrier material of nickel.

Electrodes were tested at 50°C and electrolyte concentrations 1 M KOH, 2 M KOH, 4 M KOH, 7 M KOH and 10 M KOH and in 7 M KOH at 25°C, 50°C, 70°C and 85°C.

Each solution was titrated to  $\pm$  0,05 mol/l. The cell is heated by a water bath. Potentials were measured with a Radiometer PHM 22 by means of a Luggin capillary with the tip placed in the centre of the electrode 1 mm from the surface. Current is supplied by an ASEA potentiostat. The reference electrode is a hydrogen electrode with nickel boride electrocatalyst in 7 M KOH at 50°C with a pressure of 2,6 bar. The high current densities obtained result in considerable measuring problems. One of these is an unavoidable voltage drop between the tip of the reference capillary and the electrode surface. This RI drop is measured by rapid breaking of the current with an Hg relay at the same time as the voltage process is recorded on a storage oscilloscope. This purely ohmic voltage drop decays faster than 1 microsecond and can be easily distinguished from the other polarization components. All measured values have been corrected for RI drop in this way. By the use of the same method, the shape of the entire decay curve has been studied by interrupting the current from the same potential several times with different time settings on the oscilloscope.

An investigation of the potential distribution in three dimensions in the electrolyte outside the electrode showed a slightly uneven current distribution with about 10 % higher current density in the middle than at the edge of the electrode disc. A capillary holder was made in the middle of the electrode. This test also showed that the distance of the capillary tip to the electrode is not important, as this is corrected by measuring the RI drop with the storage oscilloscope.

### 2.3

#### Electrode preparation

Hydrophilic oxygen electrodes with a diameter of 35 mm and a thickness of about 1,8 mm were made with silver electrocatalyst, palladium electrocatalyst and platinum electrocatalyst, and 95 weight % nickel. The preparation comprises pressing and sintering a mixture of nickel and electrocatalyst. The content of electrocatalyst in the active layer is 5,0 weight %. The electrodes for electrocatalytic testing were provided with a fine porous layer on the electrolyte side. This layer does not contain any electrocatalyst.

## EXPERIMENTAL RESULTS

## 3.1

Physical Properties of Electrodes with silver, palladium and platinum electrocatalyst

The thickness of the active layer was 1600 microns and the thickness of the fine layer was 200 microns.

BET surface area and porosity were measured for the active layers and listed in tabel 1.

Table 1. BET surface area and porosity for different active layers

<u>Electrode material</u>	<u>BET m<sup>2</sup>/g</u>	<u>Porosity %</u>
95 % Ni, 5 % Ag	0,19	43,4
" " "	0,15	44,1
" " "	<u>0,14</u>	<u>43,4</u>
95 % Ni, 5 % Ag, average	0,16	43,6
95 % Ni, 5 % Pd	0,19	44,6
" " "	<u>0,20</u>	<u>44,9</u>
95 % Ni, 5 % Pd, average	0,20	44,8
95 % Ni, 5 % Pt	0,14	45,9
" " "	<u>0,10</u>	<u>46,2</u>
95 % Ni, 5 % Pt, average	0,12	46,1
100 % Ni	0,14	44,2
"	0,13	44,4
"	<u>0,13</u>	<u>44,5</u>
100 % Ni, average	0,13	44,4

The majority of the surface area in the active layer consists of the supporting material nickel. Electrodes with palladium have the highest electrocatalyst surface area, followed by silver and platinum.

Electrodes with platinum electrocatalyst have a slightly higher porosity than the other electrodes.

Spot analysis with an electron microsond showed, that the electrocatalysts silver, palladium and platinum are present as pure metals in the electrode structure and not alloyed with nickel.

The electrocatalysts are evenly distributed over the thickness of the active layer. Platinum has sintered to form particles up to 5 microns while silver and palladium are considerably smaller. This explains the low BET-surface of the electrodes with platinum.

### 3.2

#### Electrochemical comparison for electrodes with Ag, Pd and Pt electrocatalysts

The variation of current density with the pressure difference between oxygen and the electrolyte at a constant polarization of -350 vs the reversible oxygen electrode was measured for electrodes with palladium and platinum electrocatalysts.

The differential pressure was increased from 0,2 atm up to 1,4 atm and down in 0,2 atm steps. Fig. 1 shows a typical curve with palladium electrocatalyst. The current density increases with differential pressure up to a maximum at 0,6 atm and then decreases.

Lindholm (3) explained this decrease in current density at higher differential pressures as a "thinning out effect" of the liquid films.

Lindström (4) measured the gas penetration into the pores and the resistance along the liquid films at varying differential pressure. He reported on an interplay between film area, film resistance and current density. At higher differential pressures, he found a further increase in gas penetration and an increase in the film resistance. It is thus apparent that the rate of mass transport of  $\text{OH}^-$  ions and  $\text{H}_2\text{O}$  along the liquid films is slower at a higher differential pressure.

The shape of these i-p curves is the same for palladium and platinum as the curves measured earlier with silver, mentioned in the First and Second Quarterly Report (1, 2).

Fig. 2 shows polarization curves at 50°C with varying electrolyte concentration from 1 M KOH to 10 M KOH for palladium electrocatalyst.

The open circuit potential is more than 200 mV from the reversible oxygen potential. At open circuit and at a low current density the diagram shows the lowest polarization for a high electrolyte concentration, 10 M KOH, and the highest polarization for a low electrolyte concentration, 1 M KOH.

At higher current densities there is a difference in the order of the polarization curves with the lowest polarization for the lowest electrolyte concentration, 1 M KOH, and increased polarization with increased KOH-concentration. They give approximatively straight lines in a linear diagram at high current density. This is the same shape of the curves as reported earlier with silver, the main differences being that the open circuit polarization is higher for palladium and that the current densities are smaller for the same potential up to about -350 mV. Platinum electrocatalyst has the same general behaviour as palladium.

Fig. 3 and 4 shows a comparison of Ag, Pd, Pt and only the nickel structure for 7 M KOH at 25° and 70°C. The nickel structure shows a high polarization already at low current densities. Silver electrocatalyst shows the lowest polarization at lower current densities. The polarization at higher current densities is about the same for all the electrocatalysts.

These data support the suggestion made in our First Quarterly Report that the surface reaction is rate-limiting at low current densities and that mass transport is rate-limiting at high current densities, giving the lowest polarization for an electrolyte with low KOH-concentration.

The rate-limiting surface reaction at low current densities and rate-limiting mass transport at high current densities exists for many reactions on a plane electrode. It is interesting to see the same behaviour in a porous electrode. This is of course influenced by the low rate constant  $i_0$  for the surface reaction.

The differences between the electrocatalysts appear at low current densities. With palladium and platinum, there is an almost straight line between 0,5 and 5 mA/cm<sup>2</sup> in a  $\eta$ -log i, diagram in accordance with Tafels formula  $\eta = a + b \log i$ , while silver has a slightly rounded curve. The b values between 0,5 and 5 mA/cm<sup>2</sup> are shown in table 2. The increase in polarization over the straight Tafel line above 5 mA/cm<sup>2</sup> is mainly due to mass transport polarization.

Table 2. b-values in mV for different electrocatalysts

M KOH	°C	Ag	Pd	Pt
1	50	49	50	56
2	50	47	48	60
4	50	44	48	62
7	50	48	48	55
10	50	50	44	52
7	25	68	45	53
7	50	48	48	55
7	70	40	40	49
7	85	36	43	43

All these b-values are around 50 mV, and the only trend is that silver has a lower b-value with an increase in temperature. This is not caused by a change of slope of a straight line, but caused by a the more curved form for silver at 25°C.

The b value has recently been measured in 1 M KOH to 60 mV for platinum by Damjanovic, Dey and Bockris (3) and in 0,1 M NaOH to 53 mV for platinum and 46 mV for palladium by Gnanamuthu and Petrocelli (4). Beer and Sandler (5) have reported that silver gives no Tafel line in pre-electrolyzed 15 % KOH solution.

Our results indicate a difference in the mechanism for oxygen reduction between silver and the other electrocatalysts - palladium and platinum.

The differences between the electrocatalysts appear at low current densities. With palladium and platinum, there is an almost straight line between 0,5 and 5 mA/cm<sup>2</sup> in a  $\eta$ -log i, diagram in accordance with Tafels formula  $\eta = a + b \log i$ , while silver has a slightly rounded curve. The b values between 0,5 and 5 mA/cm<sup>2</sup> are shown in table 2. The increase in polarization over the straight Tafel line above 5 mA/cm<sup>2</sup> is mainly due to mass transport polarization.

Table 2. b-values in mV for different electrocatalysts

M KOH	°C	Ag	Pd	Pt
1	50	49	50	56
2	50	47	48	60
4	50	44	48	62
7	50	48	48	55
10	50	50	44	52
7	25	68	45	53
7	50	48	48	55
7	70	40	40	49
7	85	36	43	43

All these b-values are around 50 mV, and the only trend is that silver has a lower b-value with an increase in temperature. This is not caused by a change of slope of a straight line, but caused by a the more curved form for silver at 25°C.

The b value has recently been measured in 1 M KOH to 60 mV for platinum by Damjanovic, Dey and Bockris (3) and in 0,1 M NaOH to 53 mV for platinum and 46 mV for palladium by Gnanamuthu and Petrocelli (4). Beer and Sandler (5) have reported that silver gives no Tafel line in pre-electrolyzed 15 % KOH solution.

Our results indicate a difference in the mechanism for oxygen reduction between silver and the other electrocatalysts - palladium and platinum.

We have earlier showed that the increase in current density with polarization  $\frac{di}{d\eta}$  is proportional vs the mass transport function  $\sqrt{SD^2}$  for silver at high polarization when the KOH-concentration is varied between 2 and 10 M and the temperature between 25 and 85°C.

This proportionality can now be extended to the other electrocatalysts. Diagram 5 shows a comparison between  $\frac{di}{d\eta}$  and  $\sqrt{SD^2}$  for palladium. This diagram includes both points for varying KOH-concentration and points for varying temperature. There is a linear dependence of  $\frac{di}{d\eta}$  with  $\sqrt{SD^2}$  at high polarization.

The dependence on temperature has been studied for electrodes with different electrocatalyst in the active layer within the most interesting temperature range, i.e. 25° - 85°C.

The exchange current density,  $i_0$ , could be calculated with Pd and Pt electrocatalysts at 25 and 50°C where a straight line was obtained.

Table 3. Exchange current density in 7 M KOH A/cm<sup>2</sup> (electrode cross section surface)

<u>Electrocatalyst</u>	<u>Pd</u>	<u>Pt</u>
25°C	$10^{-9}$	$10^{-8}$
50°C	$10^{-8}$	$10^{-7}$

The real electrocatalyst surface area is about 100 cm<sup>2</sup>/cm<sup>2</sup> cross section for Pt. The value of  $i_0$  for real electrocatalyst area at 25°C about  $10^{-10}$  A/cm<sup>2</sup> for Pt and about  $2 \cdot 10^{-12}$  A/cm<sup>2</sup> for Pd from our measurements. These values can be compared with  $3 \cdot 10^{-10}$  A/cm<sup>2</sup> in 1 M KOH measured by Damjanovic et al (5) and  $10^{-10}$  A/cm<sup>2</sup> for Pt and  $10^{-12}$  A/cm<sup>2</sup> for Pd in 0,1 M NaOH measured by Gnanamuthu and Petrocelli (6).

Fig. 6 shows polarization curves for platinum in 7 M KOH at different temperatures. The polarization decreases with increased temperature. At high current densities there is a tendency towards limiting current density for the lower temperatures.

We have earlier showed that the increase in current density with polarization  $\frac{d_i}{d\eta}$  is proportional vs the mass transport function  $\sqrt{SDP}$  for silver at high polarization when the KOH-concentration is varied between 2 and 10 M and the temperature between 25 and 85°C.

This proportionality can now be extended to the other electrocatalysts. Diagram 5 shows a comparison between  $\frac{d_i}{d\eta}$  and  $\sqrt{SDP}$  for palladium. This diagram includes both points for varying KOH-concentration and points for varying temperature. There is a linear dependence of  $\frac{d_i}{d\eta}$  with  $\sqrt{SDP}$  at high polarization.

The dependence on temperature has been studied for electrodes with different electrocatalyst in the active layer within the most interesting temperature range, i.e. 25° - 85°C.

The exchange current density,  $i_0$ , could be calculated with Pd and Pt electrocatalysts at 25 and 50°C where a straight line was obtained.

Table 3. Exchange current density in 7 M KOH A/cm<sup>2</sup> (electrode cross section surface)

<u>Electrocatalyst</u>	<u>Pd</u>	<u>Pt</u>
25°C	$10^{-9}$	$10^{-8}$
50°C	$10^{-8}$	$10^{-7}$

The real electrocatalyst surface area is about 100 cm<sup>2</sup>/cm<sup>2</sup> cross section for Pt. The value of  $i_0$  for real electrocatalyst area at 25°C about  $10^{-10}$  A/cm<sup>2</sup> for Pt and about  $2 \cdot 10^{-12}$  A/cm<sup>2</sup> for Pd from our measurements. These values can be compared with  $3 \cdot 10^{-10}$  A/cm<sup>2</sup> in 1 M KOH measured by Damjanovic et al (5) and  $10^{-10}$  A/cm<sup>2</sup> for Pt and  $10^{-12}$  A/cm<sup>2</sup> for Pd in 0,1 M NaOH measured by Gnanamuthu and Petrocelli (6).

Fig. 6 shows polarization curves for platinum in 7 M KOH at different temperatures. The polarization decreases with increased temperature. At high current densities there is a tendency towards limiting current density for the lower temperatures.

The electrodes give an approximatively linear relationship between log current density at a given polarization and  $1/T$  from which an activation energy can be calculated which comprises the whole reaction cycle.

Fig. 7 shows a comparison from the polarization curves of the reaction rate - the current density - at a low polarization of 300 mV and a high polarization of 500 mV. The activation energy from fig. 6 is shown in tabel 4.

Tabel 4 Activation energy for oxygen reduction in 7 M KOH at -300 and -500 mV vs reversible oxygen potential in same solution kcal/mole, temperature range 25 - 85°C

	<u>-300 mV</u>	<u>-500 mV</u>
Silver	8,4	5,8
Palladium	7,8	4,4
Platinum	8,0	4,7

The higher activation at a low polarization for all electro-catalysts supports the conclusion that the surface reaction is rate-limiting at a low polarization with a high activation energy and that mass transport is rate-limiting at higher current densities giving a lower activation energy.

The calculated activation energy for a theoretical expression of the rate of mass transport,  $\sqrt{SD\mathcal{R}}$ , is 5,0 kcal which is very near our measured values at 500 mV polarization. This expression is from Austins "thin-film theory" (8)

$$i = \sqrt{SD\mathcal{R}} \sqrt{2nFA/w} \sqrt{\eta_s - \eta_o}$$

S = oxygen solubility in KOH

D = oxygen diffusivity in KOH

$\mathcal{R}$  = conductivity in KOH

### 3.3

#### The decay of polarization with time for Ag, Pd and Pt electrocatalysts

There are many transient methods available to study electrochemical reactions, but it is rather difficult to apply these methods to porous electrodes, the main difficulty being the potential distribution in the liquid films, while the potential is measured in the bulk solution. We have chosen the potential decay method which is a straight forward approach to the problem.

We have measured the decay of polarization after current interruption with the different electrocatalysts.

The process after current interruption is a combination of internal short-circuit currents with surface reactions, changement in double layer capacity, diffusion of  $O_2$  through the liquid film and diffusion of  $OH^-$  and  $H_2O$  along the liquid films, electrosorption of oxygen and decomposition of  $HO_2^-$ . These processes give an equilibrium at steady state. These processes are schematically shown in fig. 8.

Fig. 9 shows decay curves for an electrode with silver electrocatalyst. The potential before interruption was -350 mV vs reversible oxygen electrode. This figure shows the effect of varying differential pressure between oxygen and the electrolyte, from 0,6 atm up to 1,4 atm. The electrode contains a significant amount of gas within the pore structure for all these pressures. The decay curves are very similiar, with a little faster decay of polarization at the highest differential pressure.

Fig. 10 gives the polarization decay for an electrode with silver electrocatalyst. The potential before interruption was -350 mV and - 500 mV vs rev.  $O_2$ , and the KOH-concentration 2 M KOH and 10 M KOH. The figure shows that the oxygen electrode in 10 M KOH decays towards a more positive value than in 2 M KOH, and that the decay from a higher polarization is faster in the beginning up to about 0,4 s after current interruption and that the curves with different polarization have the same rate of decay after 0,4 s.

Fig. 11 shows a comparison of polarization for Ag, Pd and Pt electrocatalysts. Silver has a faster decay of the polarization, and reaches a more positive potential than platinum and palladium. All decay curves give straight line in a  $\eta$  -logt diagram from 0,001 s up to a certain time where the slope becomes steeper. This linear portion is considerably shorter for silver than for the other electrocatalysts.

The total process after current interruption can be divided in the following stages:

1. Short circuit currents (fast)
2. Diffusion of  $O_2$  through the liquid film (relatively fast)
3. Diffusion of  $OH^-$ ,  $K^+$  and  $H_2O$  along the film (slow)
4. Electrosorption of oxygen
5. Peroxide decomposition (chemical or electrochemical)

The rate of stage 1, 2 and 3 should not differ very much for different electrocatalysts.

The short circuit currents are the main part in the first straight line decay of polarization while the latter part is caused from the slower processes. The difference between the electrocatalysts can be explained by either:

1. Faster electrosorption of oxygen on silver or
2. Faster peroxide decomposition on silver.

It is not possible to separate these two with this experimental material.

The surface area for electrodes increases in the order  $Pt < Ag < Pd$ . This difference could influence the Pt curve.

Fig. 12 shows the influence of temperature of the polarization decay from -350 mV for platinum. An increase in temperature gives a steeper slope on the first straight line, and a change to a steeper slope at an earlier time. The rate of decay is about 50 times faster at  $80^\circ C$  compared with  $25^\circ C$ . This large change in the rate of decay cannot be explained by differences in mass transport properties.

A surface reaction with a high activation energy or a combination of different surface reactions are the rate-limiting stages in the decay of polarization

## 3.4

Pore structure

The pore structure has been investigated with the experimental technique described by Lindström (4). This technique comprises a method to measure the relative amount of gas and liquid in the pores at varying differential pressure by means of a gas porosimeter. The surface area of the liquid film in the pores is calculated from this data with a computer (GE 625). The resistance along the liquid films is measured with a special electrode layer containing an active pore layer in the middle and a fine pore on each side. This electrode is filled with electrolyte in a special test cell and the resistance between the different sides of the electrode is measured by reference electrodes when a current is passed through the electrolyte. The current is selected to a low value when all the conductivity through the electrode is via the electrolyte. A nitrogen gas pressure is applied from the cylindrical area of the electrodes, and the resistance along the liquid films can be measured at varying differential pressures.

These experiments were performed with silver electrocatalyst with a 1600 microns deep active layer, 7 M KOH at 50°C.

The amount of gas in the pore system is shown in fig. 13, and the calculated film surface area in fig. 14.

The resistance along the liquid films with varying differential pressure is shown in fig. 15. When the resistance along the films and the content of electrolyte in the pores are known, it is possible to calculate a tortuosity factor,  $K_t$ . This factor is defined as the ratio of the measured resistance in the liquid film to a calculated resistance for the same amount of liquid in a straight pore without bends and area restrictions.

Fig. 16 shows the relative conductivity in the liquid films as a function of the amount of liquid in the pore volume. The tortuosity factor was measured to 1,84 when all pores are filled with electrolyte. The relative film conductivity is lowered more than calculated from the smaller content of liquid in the pores. This is due to an increase in the tortuo-

Fig. 17 shows the film area, relative conductivity of the film, and current density at -350 mV polarization vs reversible oxygen electrode in 7 M KOH and 50°C as a function of the differential pressure. These curves were measured in three separate measurements. The current density first increases with increasing differential pressure due to increased film area, reaches an optimum and then decreases due to the decreased film conductivity.

4

## OXYGEN REDUCTION, DIFFERENT ELECTROCATALYSTS. DISCUSSION

### 4.1

#### General

Our experiments have shown a difference between silver and the platinum metals at low current density giving a lower polarization for silver electrocatalyst. A literature search was made to find out possible differences and an explanation why silver gives a lower polarization.

Much of the effort in current electrochemical research is devoted to the elucidation of the mechanism of the oxygen electrode, however most of this work refers to oxygen evolution or reduction in an acid solution. Ideally, the reaction at the oxygen electrode in alkaline electrolyte would be

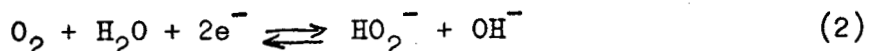


At 25°C this reaction should take place at a potential of 1.23 volt vs a reversible hydrogen electrode but it is not yet possible to make electrodes that can reach this potential and sustain current near the theoretical potential in alkaline solution.

### 4.2

#### Reaction mechanism on carbon

Berl (9) showed that hydrogen peroxide was an intermediate in the reduction of oxygen on carbon electrodes in alkaline electrolyte where the potential is determined by the reaction

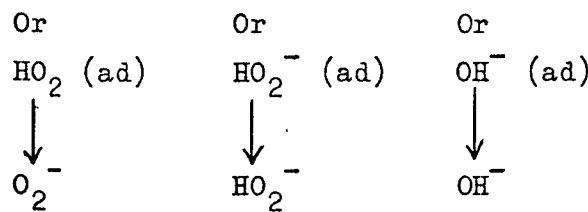
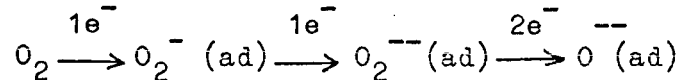


The electrode potential is:

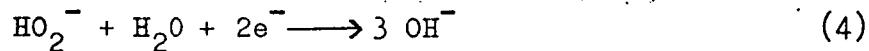
$$E = E^{\circ} - \frac{RT}{2F} \ln \frac{a_{\text{OH}} - a_{\text{HO}_2^-}}{a_{\text{O}_2} a_{\text{H}_2\text{O}}}$$

Davies, Clark, Yeager and Hovorka (10) showed with isotope experiments that the O-O bond is not broken during the reac-

Yeager (9) summarizes the mechanism in alkaline electrolyte in this scheme:



When  $\text{HO}_2^-$  is formed in a 2-electron reaction, it can be further reduced either electrochemically,



or be decomposed catalytically



The oxygen is further reduced electrochemically so that the total amount of electrons is 4. Yeager has worked with carbon electrons of high density. He showed (11,12) that oxygen reduction on carbon in a 2-electron process with  $\text{HO}_2^-$  as an intermediate and that the function of a silver catalyst on carbon is to promote the decomposition of the peroxide.

#### 4.3

##### Reaction mechanism on metals

The reaction mechanism for oxygen reduction on metals has received much attention. Damjanovic, Dey and Bockris (5) and Gnanamuthu and Petrocelli (6) have listed 16 different reaction paths, each path with different steps which might be rate-determining. The slope of the Tafel line is due to the rate-determining step, and the theoretical slope has been calculated for each step.

The intermediate stages in these paths are peroxide, and oxygen adsorbed in molecular or atomic form or in surface oxides. One of the main difficulties in determining the mechanism is that several steps have the same theoretical

Tafel slope. The path and r.d.s. can be changed with varying electrolyte, electrocatalyst and potential. The situation can be further complicated by side reactions.

Hydrogen peroxide has been detected when oxygen is reduced on nickel (12), platinum (12, 13, 14), gold (15) and silver (16).

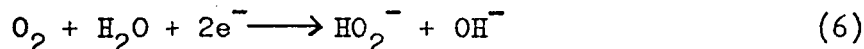
Damjanovic, Genshaw and Bockris (13) conclude that oxygen reduction on platinum in alkaline solution occurs in two paths simultaneously at comparable rates. One of these two paths has hydrogen peroxide ( $\text{HO}_2^-$ ) formed as an intermediate which partially reduces further at the electrode.

Shumilova et al (16) reduced oxygen on smooth silver in alkaline electrolyte and found hydrogen peroxide at 0,85 V vs hydrogen electrode. With the potential shifting in the cathodic direction, a sharp decrease in the hydrogen peroxide yield occurred.

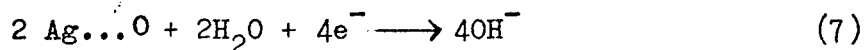
Vielstich and Mrha (17) have studied the change in potential with oxygen pressure

$$\frac{d\phi}{d \log P_{\text{O}_2}}$$

at very low cathodic currents with silver catalyzed carbon electrodes, and found an electron consumption of 2.6 in the first step per  $\text{O}_2$  molecule at current densities  $< 1\mu\text{A}/\text{cm}^2$ . This result is explained by the simultaneous occurrence of the Berl reaction (electron consumption 2 per  $\text{O}_2$  molecule).



and the reduction of chemisorbed oxygen (electron consumption 4 per  $\text{O}_2$  molecule)



#### 4.4

##### Hydrogen peroxide decomposition

The decomposition of hydrogen peroxide is favored by strong alkaline solution, temperature and electrocatalysts like

received surprisingly little attention (18) and we have not found an experimental comparison in the literature between silver, palladium and platinum with the surface reaction rate-determining.

Smith et al (19) have measured the open-circuit potentials for silver, palladium and platinum in 5 M KOH, 1 M  $H_2O_2$  at 30°C. They found -250 mV from reversible oxygen potential for silver and - 340 mV for palladium and platinum. The electrodes could be loaded up to about  $100 \text{ mA/cm}^2$  with little additional polarization. The difference between silver and the platinum metals is 90 mV. If this potential difference is due to differences in  $HO_2^-$  concentration at the electrode surface, this means 1000 times lower  $HO_2^-$  concentration on Ag than Pt.

Hurlen et al (20) have studied hydrogen peroxide decomposition in 1 M KOH containing 0,1 M  $H_2O_2$  at 25°C. The initial constant rate is  $0,04 - 0,08 \text{ ml O}_2/\text{cm}^2/\text{min}$ . which is equivalent to the limiting diffusion current. The peroxide decomposition from an originally very low concentration near the electrode surface is of course difficult to study directly on different electrode materials.

#### 4.5

##### Adsorption on the electrode surface

Chemisorption of oxygen and oxide formation are thermodynamically possible for silver, palladium, platinum and nickel in contact with oxygen.

Wroblowa, Rao, Damjanovic and Bockris (21) have recently published a paper on electrosorption of oxygen at a platinum electrod in acid solution. Other platinum metals has also been studied in acid solution (22).

Electrosorption of oxygen in alkaline solution has not received much attention, and we have not been able to find a direct comparison between silver, platinum and palladium.

Investigations of adsorption of oxygen from gas phase (without electrolyte) have shown differences between silver and

platinum. Bond (18) has tabulated the electronegativity of the adsorbed oxygen (in atom form), the surface potential, which is -0,2 V for silver, -1,1 to 1,2 V for platinum, -0,9 to -1,25 V for palladium and -1,4 to -1,6 V for nickel reflecting differences in the oxygen - metal bond.

Sandler (23) has studied oxygen adsorption from gas phase. He concludes that at least two types of chemisorption exist on silver, presumably differing in their coordination with silver atoms. Some strongly bound oxygen is also occluded below the surface. Czanderna (24) has also studied adsorption from gas phase and conclude that both atomic and molecular oxygen exist on a silver surface.

The main difference between adsorption in gas phase and adsorption from solution, is that adsorption of oxygen dissolved in the electrolyte is a replacement reaction where the oxygen replaces water or other species. A monograph on electrosorption has recently been published by Gileadi (25).

The electrosorption of oxygen is competing with several other species, including  $H_2O$ ,  $OH^-$ ,  $K^+$  and  $HO_2^-$ . The electrosorption is influenced by the potential of zero charge, which is about -0,45 V for silver and +0,35 V for platinum (25). These data have not been measured in strong alkaline solution, and they will be shifted both by adsorption of  $OH^-$  adsorption of oxygen and possibly absorption in silver of oxygen. The measured values indicate, however, a difference in potential of zero charge between silver and platinum.

The large differences in oxygen adsorption from gas phase on silver and platinum as well as the differences in potential of zero charge indicate that large differences in oxygen electrosorption on silver and platinum are possible.

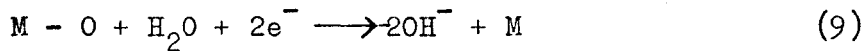
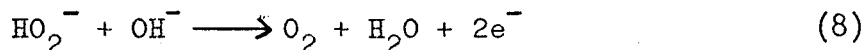
#### 4.6

##### Open circuit potential

The reversible oxygen potential has not yet been reached on any electrode material in alkaline solution at 25°C.

Hoare (26) made an oxygen electrode reversible in acid solution by treating platinum with  $\text{HNO}_3$  to form a special oxide. Sandler (23) tried this electrode treatment in alkaline solution, but did not find the reversible potential and no major difference in potential when comparing with untreated platinum.

The open-circuit potential is assumed to be a mixed potential from the reactions (27):



There are two main possibilities reach a more positive value from this mixed potential:

1. The surface concentration of hydrogen peroxide ions is lowered by means of decomposition.
2. The electrosorption of oxygen occurs in way that increases the chemical potential of adsorbed oxygen.

The difference in behavior between silver and the platinum metals is due to one of these possibilities. The peroxide decomposition possibility means that silver lowers the peroxide ion concentration to about  $10^{-9}$  M and platinum and palladium to  $10^{-7} - 10^{-8}$  M at  $0,5 \text{ mA/cm}^2$  for a porous electrode.

#### 4.7

##### Comparison at high polarization

Hartner, Vertes, Medina and Oswin (28) studied oxygen reduction on flat plates of platinum, palladium, silver and gold in 5 M KOH at  $25^\circ\text{C}$ . At a high polarization of 800 mV they found that the current increased with oxygen pressure but was independent of the electrode material. The surface reaction including hydrogen peroxide decomposition is very rapid at high polarization and mass transport is rate-limiting. This is in agreement with our results in this report for silver, palladium and platinum.

## 4.8

Comparison with mathematical treatments of the "Thin-film model"

The "Thin-film model" of porous gas-diffusion electrodes was first treated by Austin et al (8). Their evaluation considers mass transport polarization through a liquid film and OH<sup>-</sup> ion transport along the film, but not the polarization caused by the surface reaction. This is a limitation in the region of low polarization where we have shown that the surface reaction is important. A more detailed treatment has recently been carried out by Srinivasan and Hurwitz (29) They have made calculations in the case where all forms of polarization - activation, mass transport and ohmic - are considered, varying the kinetic and physical parameters.

Fig. 19 compares the numerical calculations according to Austin et al, the numerical calculations according to Srinivasan and Hurwitz (29) which also considers activation polarization, and our experimental values for silver, palladium and platinum electrocatalysts in 4 M KOH at 50°C.

The shape of the experimental curves is different from the calculated curve according to Austin et al, but similar to the curve calculated by Srinivasan and Hurwitz. This indicates again the strong influence from the surface reaction on the polarization at low current densities. The agreement between the measured experimental curves and the numerical calculations of Srinivasan and Hurwitz is good, considering the differences in physical parameters and some differences between the model and a real porous electrode, e.g. uneven liquid films introducing a tortuosity factor.

Table 5 compares the numerical values used by Srinivasan and Hurwitz with our experimental data.

Table 5. Kinetic and physical parameters

	$DnFc^0$ A/cm	$\delta'$ $\text{ohm}^{-1}\text{cm}^{-1}$	$r_2$ cm	$\Delta_r$ cm
Srinivasan and Hurwitz	$10^{-6}$	1	$10^{-4}$	$10^{-5}$
Experimental conditions	$3 \cdot 10^{-6}$	0,75	$3 \cdot 10^{-4}$	$10^{-4}$

$c^0$  = concentration of reactant

$r_2$  = radius of the pore

$\Delta_r$  = film thickness

Srinivasan and Hurwitz used an exchange current density of  $10^{-6}$  A/cm<sup>2</sup> in their calculations. The exchange current density for oxygen reduction is considerably lower than  $10^{-6}$  A/cm<sup>2</sup>. According to Bockris (30) the calculated curve must be transposed towards an increased polarization. We have shifted the curve 0,18 V to account for the lower exchange current density.

## CONCLUSIONS AND FUTURE PLANS

Silver, palladium and platinum electrocatalysts in porous nickel have a different behaviour in electrochemical reduction of oxygen.

Silver has a lower polarization from the reversible oxygen electrode than palladium and platinum at open circuit and at a low current load. This difference is either due to differences in electrosorption of oxygen or to differences in hydrogen peroxide ion ( $\text{HO}_2^-$ ) decomposition rate.

The rate of oxygen reduction at high polarization is approximately the same for these catalysts and determined by mass transport of  $\text{O}_2$  through the liquid film and  $\text{OH}^-$  along the film. The inverse slope of the polarization curve at high polarization  $\frac{d_i}{d\eta}$  is proportional to the mass transport function  $\sqrt{\text{SDR}}$ .

The decay of polarization after current interruption is faster with silver electrocatalyst than platinum and palladium. The reason is again either faster peroxide decomposition or a difference in electrosorption.

Future plans include measurements with gas mixtures,  $\text{O}_2 - \text{Ar}$  and  $\text{O}_2 - \text{He}$  to study mass transport in gas phase by mixed diffusion technique.

## LIST OF REFERENCES

1. Lindholm, I, Edwardsson, I:  
NASW-1536. First Quarterly Report April 1 - June 30, 1967
2. Lindholm, I, Edwardsson, I:  
NASW-1536. Second Quarterly Report July 1 - Sept 30, 1967
3. Lindholm, I:  
Deuxieme Journées Internationales d'Etude des Piles à Combustibles. Bruxelles June 1967
4. Lindström, O:  
Natl Meeting Am. Chem. Soc. Div. of Fuel Chem. Sept 1967
5. Damjanovic, A, Dey, A, Bockris, J O' M:  
J Electrochem. Soc. 113(7)739 1966
6. Gnanamuthu, D S, Petrocelli, J V:  
J Electrochem. Soc. 114(10)1036 1967
7. Beer, S Z, Sandler, Y L:  
J Electrochem. Soc. 112(11)1133 1965
8. Austin, L G, Ariet, M, Wood, G B, Walker, R D, Comyn, R H:  
Ind. Eng. Chem. Fundamentals 4 321 1965
9. Berl, W:  
Trans. Electrochem. Soc. 83 253 1943
10. Davies, M, Clark, M, Yeager, E, Hovorka, F:  
J Electrochem. Soc. 106 56 1959
11. Yeager, E:  
XVII CITCE-meeting, Tokyo 1966
12. Yeager, E, Kozawa, A:  
Kinetic Factors in Fuel Cell Systems. The Oxygen Electrode Contract Nonr 2391(00) 1964

13. Damjanovic, A, Genshaw, M A, Bockris, J O'M:  
*J Phys. Chem.* 70(11)3761 1966
14. Bagotzky, V S:  
Fifth International Power Sources Symposium, Brighton 1966
15. Damjanovic, A, Genshaw, M A, Bockris, J O'M:  
*J Electroanal. Chem.* 15 173 1967
16. Shumilova, N A, Tarasevich, M R, Zhutaeva, G V:  
XV CITCE-meeting, London 1964
17. Vielstich, W, Mrha, J:  
Fifth International Power Sources Symposium, Brighton  
sept. 1966
18. Bond, G C:  
*Catalysis by Metals.* London 1962
19. Smith, J O, Gentile, R G, Leitz, F B, Sama, D A:  
Contract No DA 19-129-QM-1698(01 5017) 1961
20. Hurlen, T, Sandler, Y L, Pantier, E A:  
*Electrochimica Acta* 11(10)1463 1966
21. Wroblowa, H, Rao, M L B, Damjanovic, A, Bockris, J O'M:  
*J Electroanal. Chem.* 15 139 1967
22. Rao, M L B, Damjanovic, A, Bockris, J O'M:  
*J Phys. Chem.* 67 2508 1963
23. Sandler, Y L:  
A Study of the Adsorption Mechanism on Oxygen Electrodes.  
Report No 3, Contract DA-36-039 AMC-00136(E) 1963
24. Czanderna, A W:  
*J Phys. Chem.* 68 2765 1964
25. Gileadi, E:  
*Electrosorption.* New York 1967

28. Hartner, A J, Vertes, M A, Medina, V E, Oswin, H G:  
Am. Chem. Soc. 145th Meeting sept 1963
29. Srinivasan, S, Hurwitz, H D:  
Electrochimica Acta 12 495 1967
30. Bockris, J O'M:  
Private Communication

FIG 1

## CURRENT DENSITY VS DIFFERENTIAL PRESSURE, PALLADIUM ELECTRO-CATALYST

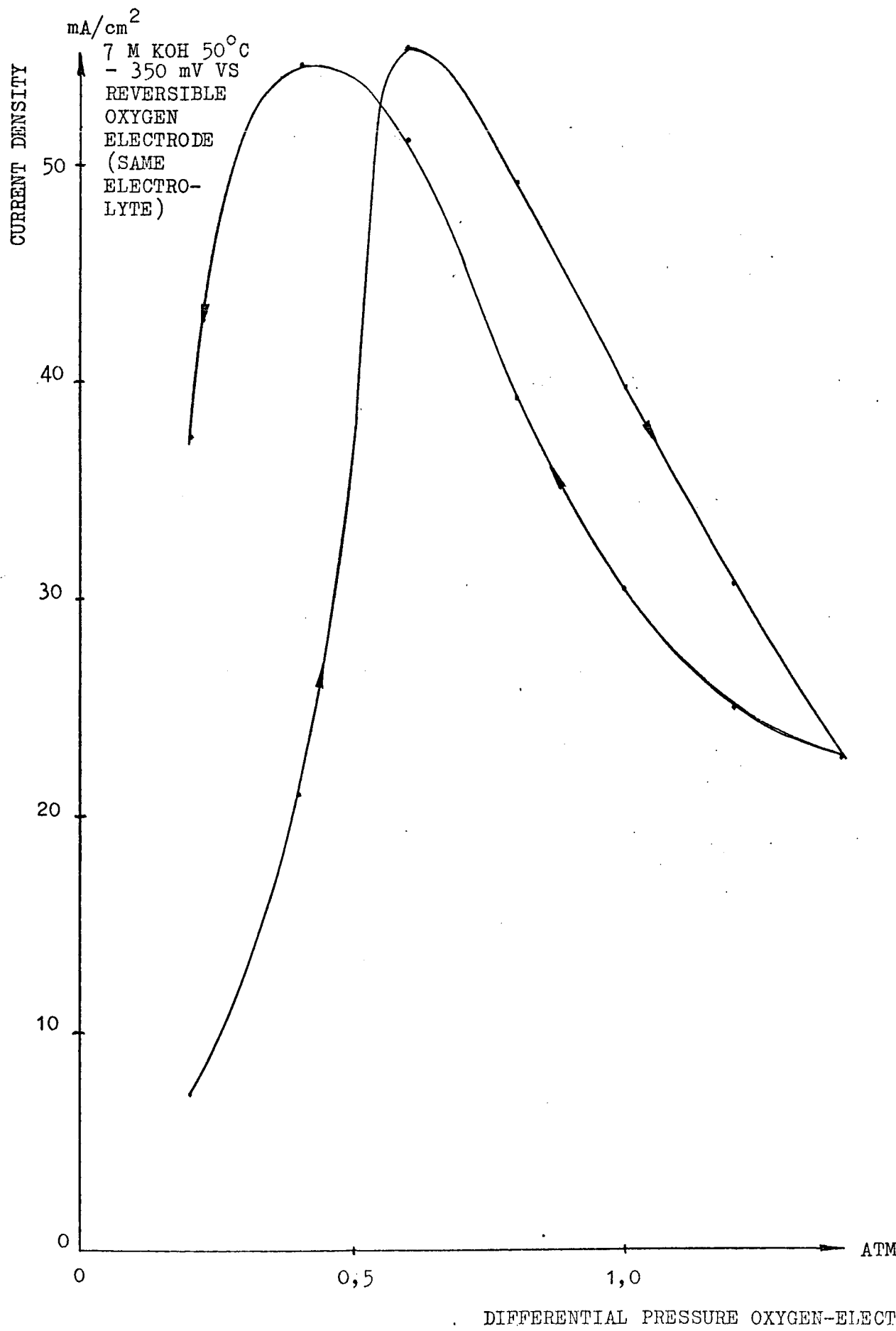


FIG 2

POLARIZATION CURVES AT OPTIMUM DIFFERENTIAL PRESSURE WITH VARYING ELECTROLYTE CONCENTRATION. PALLADIUM ELECTROCATALYST

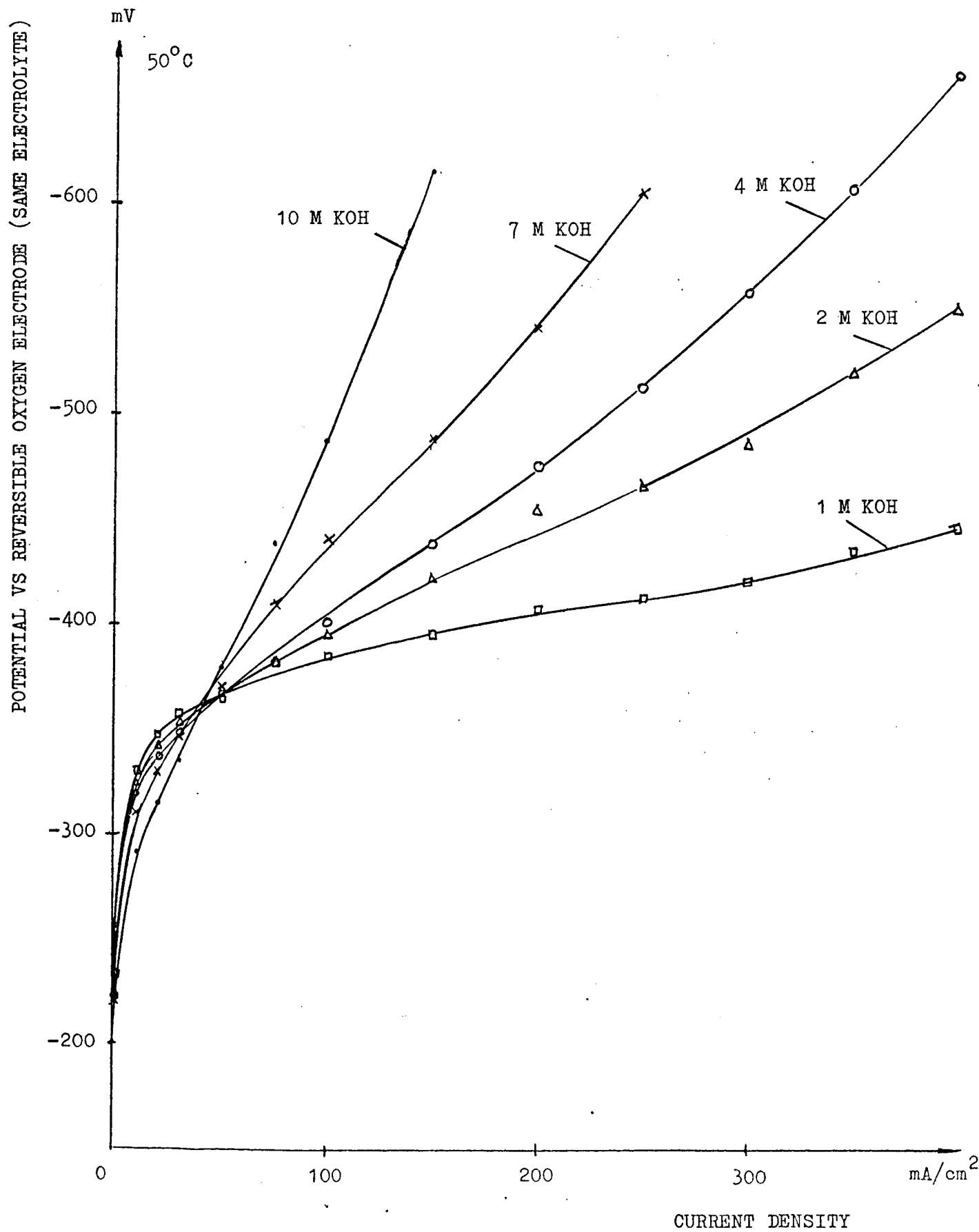


FIG. 3

POLARIZATION CURVES AT OPTIMUM DIFFERENTIAL PRESSURE FOR Ag, Pd and Pt ELECTROCATALYSTS COMPARED WITH A NICKEL STRUCTURE

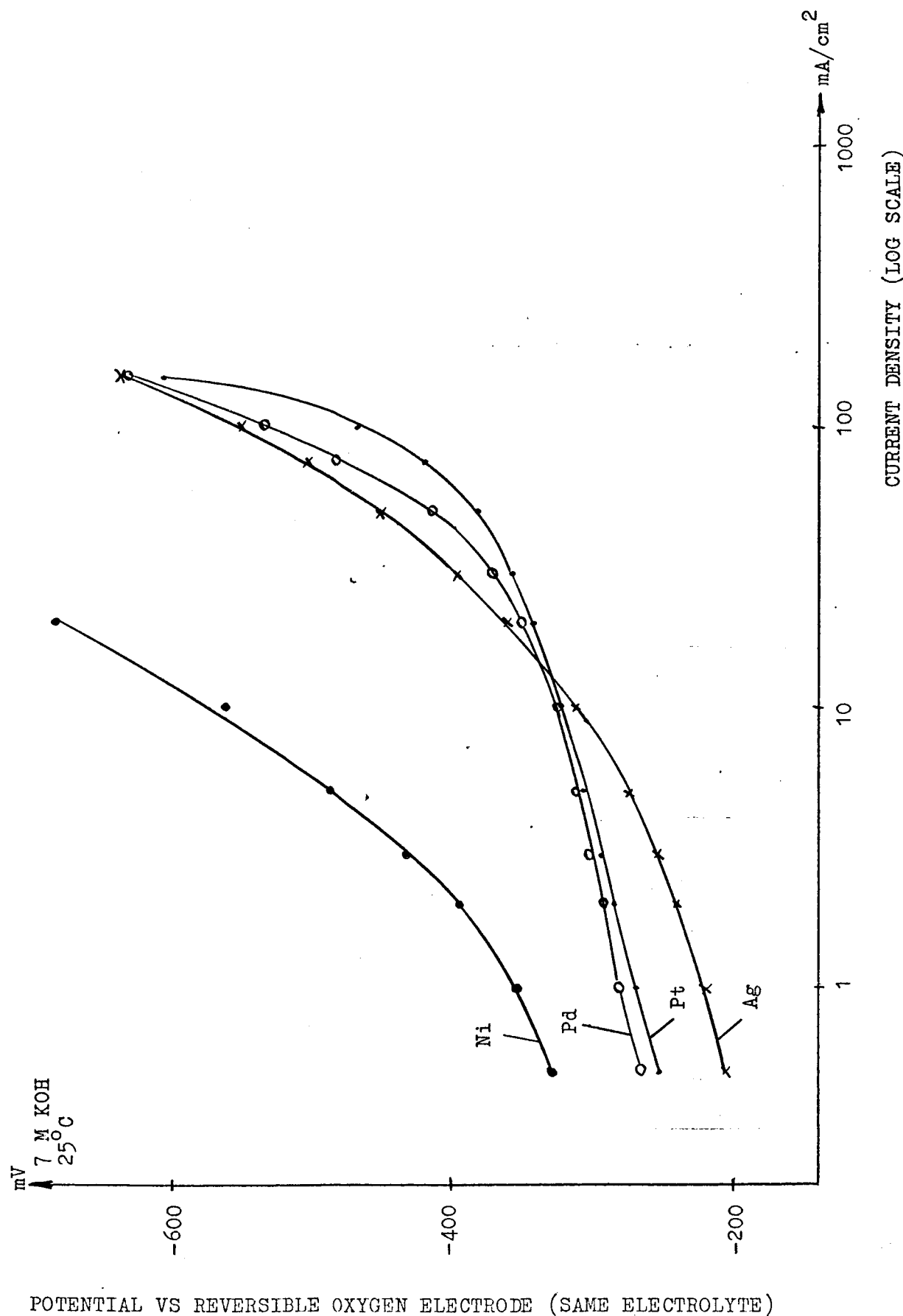
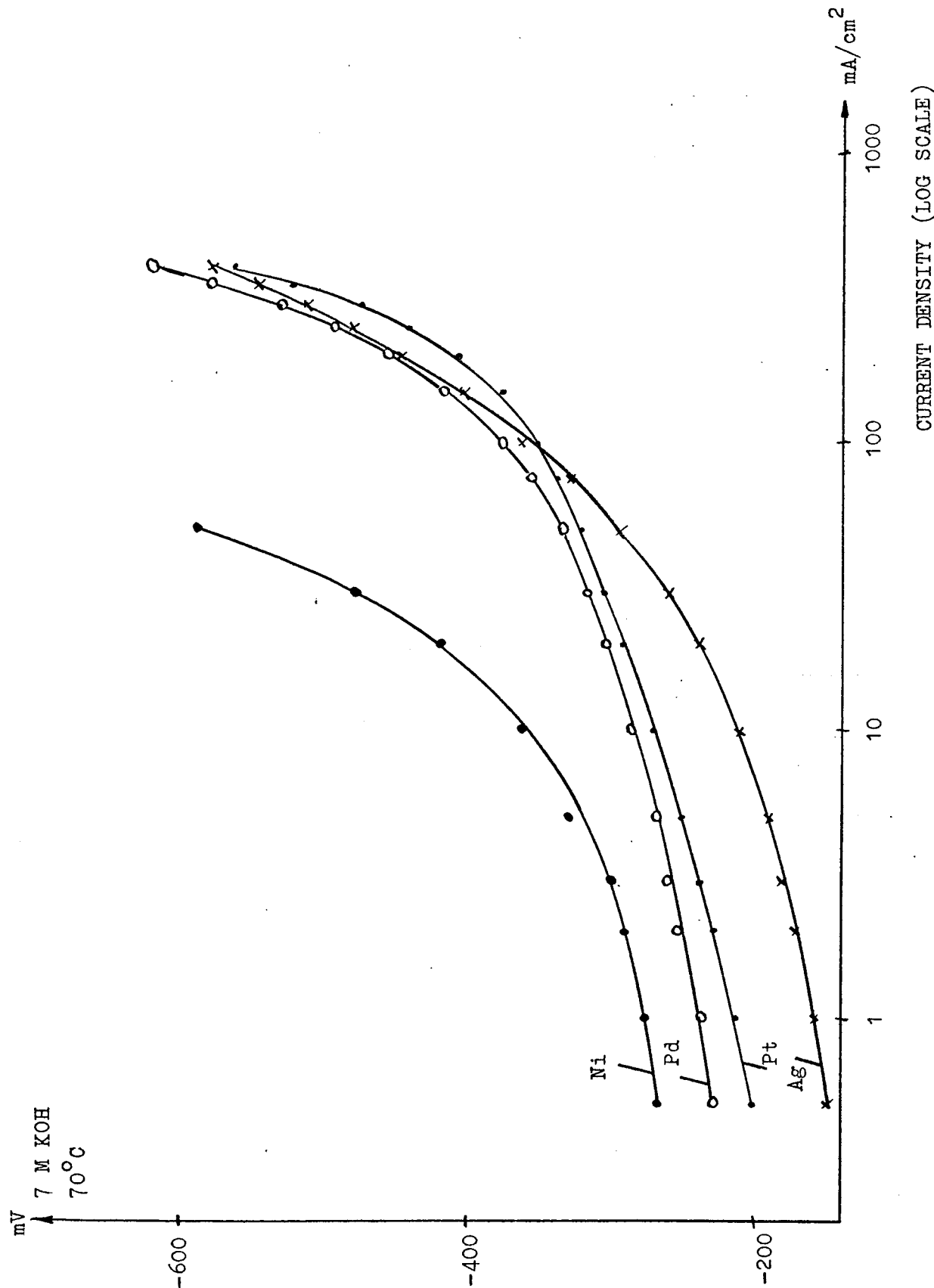


FIG 4

POLARIZATION CURVES AT OPTIMUM DIFFERENTIAL PRESSURE FOR Ag, Pd and Pt ELECTROCATALYSTS COMPARED WITH A NICKEL STRUCTURE



POTENTIAL VS REVERSIBLE OXYGEN ELECTRODE (SAME ELECTROLYTE)

FIG 5

COMPARISON BETWEEN THE INVERSE SLOPE OF THE POLARIZATION CURVE

$$\frac{di}{d\eta}$$

AT A HIGH POLARIZATION AND A MASS TRANSPORT FUNCTION  $\sqrt{SD\alpha}$  CALCULATED FOR KOH ELECTROLYTE. PALLADIUM ELECTROCATALYST

$$\Omega^{-1} \text{cm}^{-2}$$

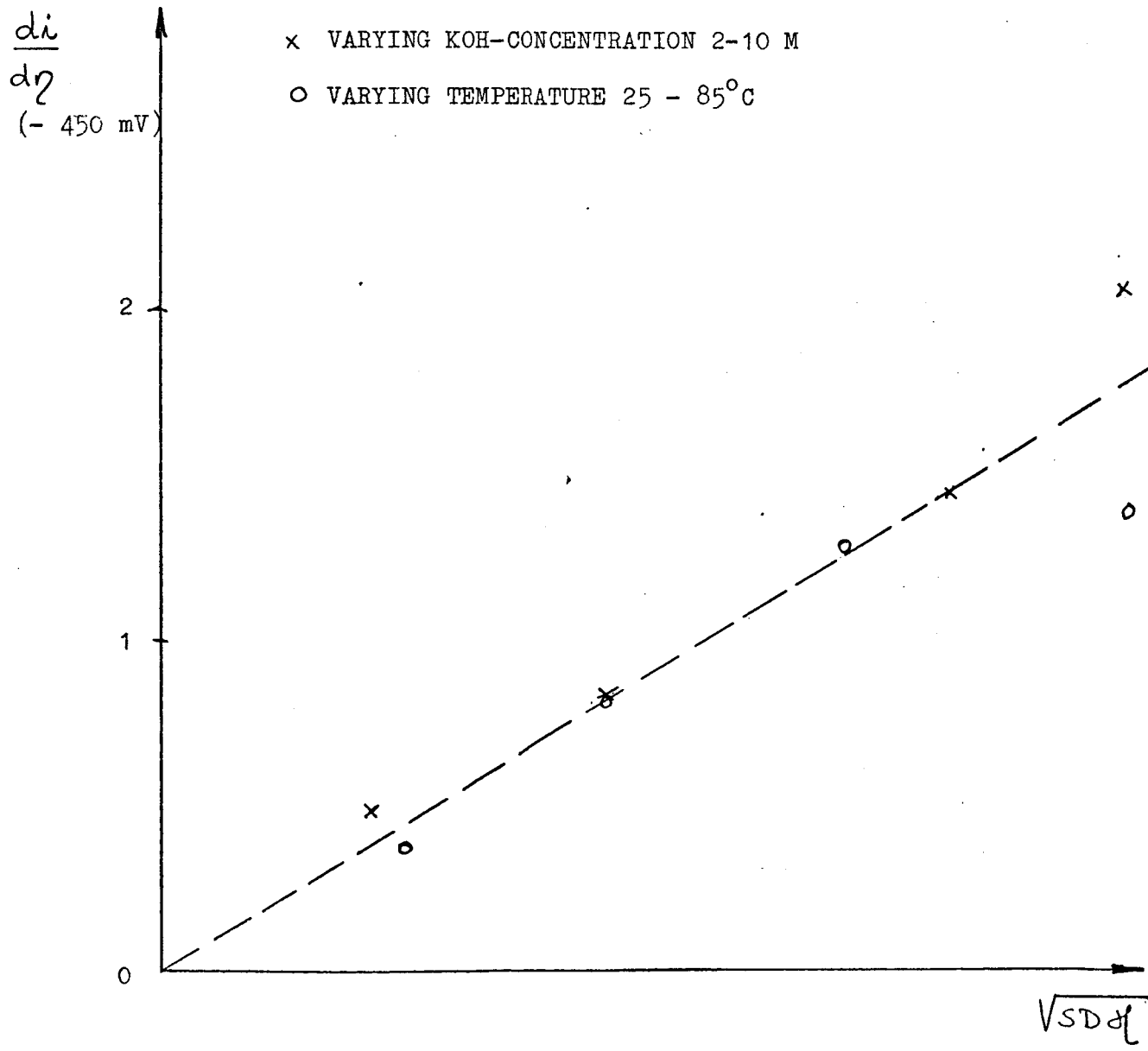


FIG 6

POLARIZATION CURVES AT OPTIMUM DIFFERENTIAL PRESSURE WITH VARYING TEMPERATURE. PLATINUM ELECTROCATALYST.

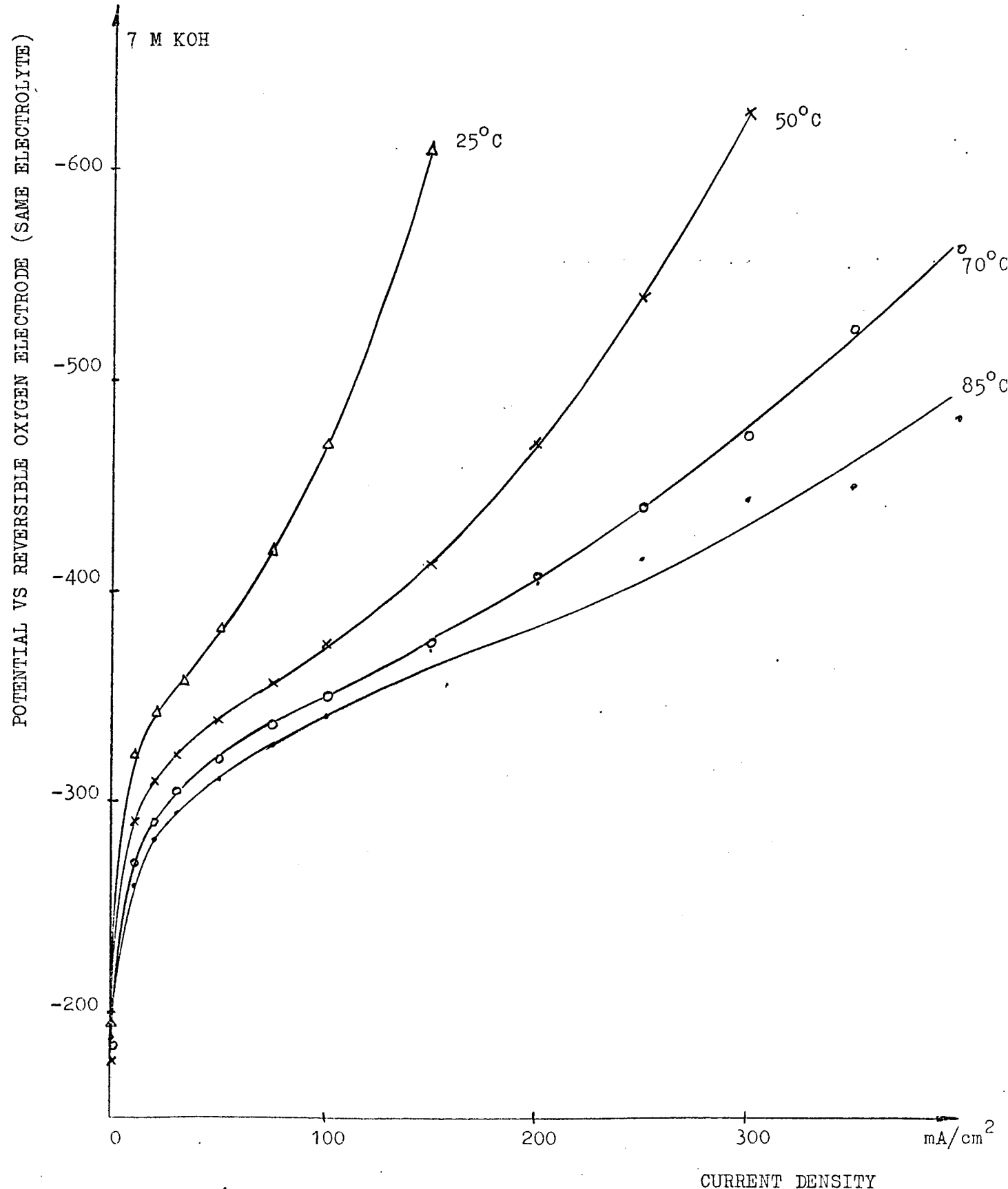
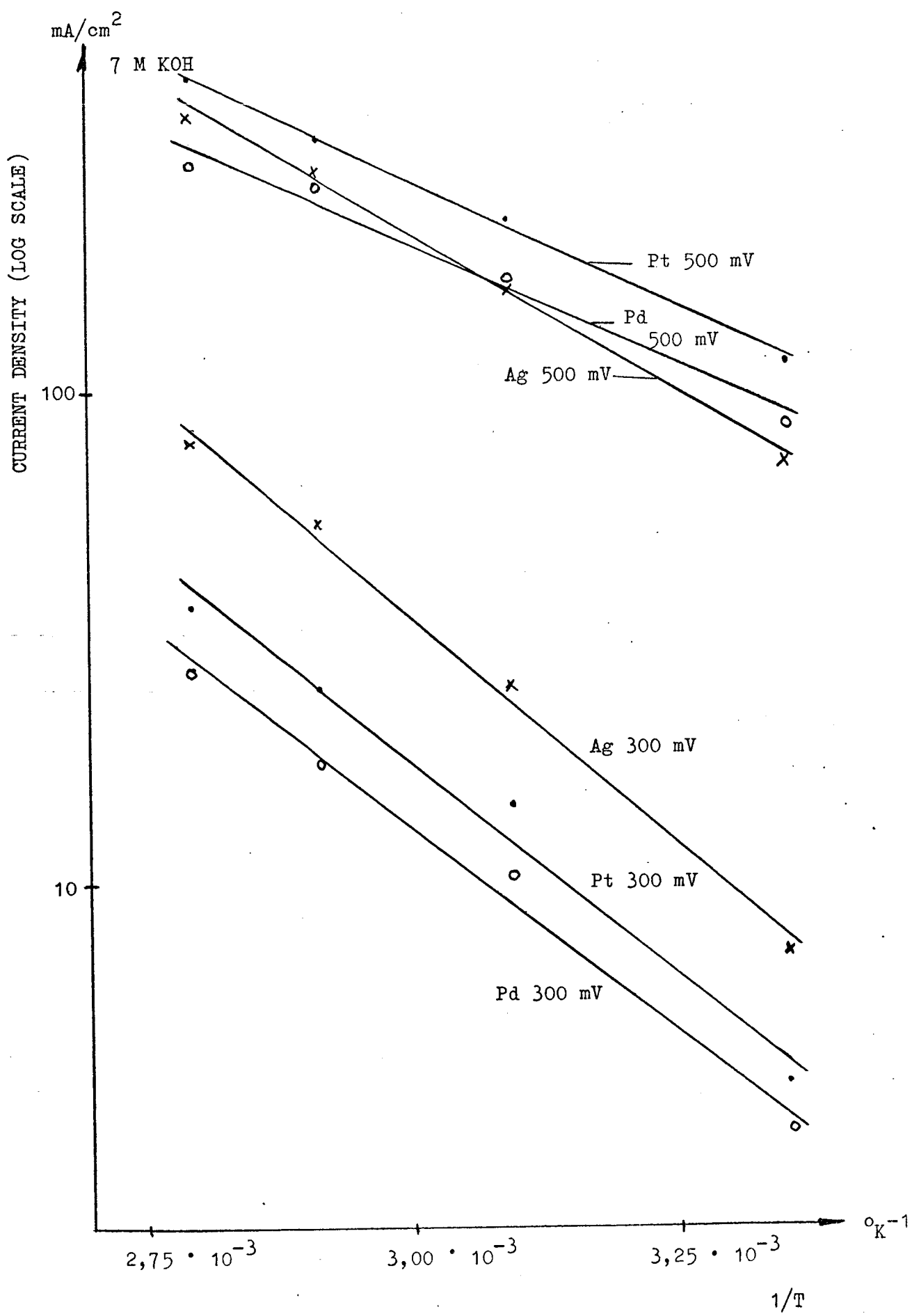


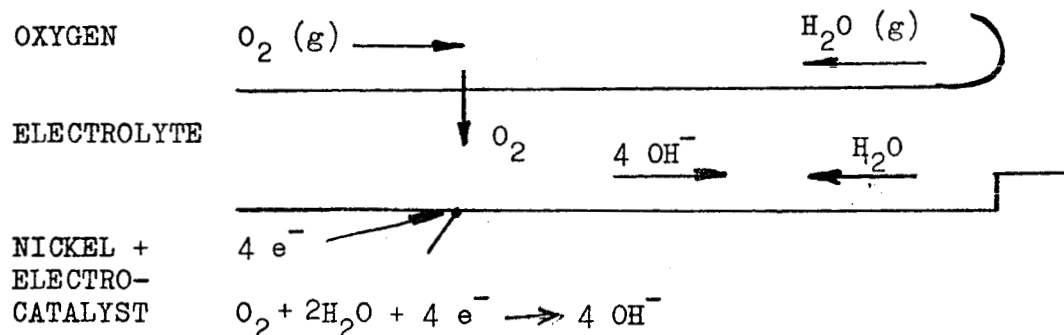
FIG 7

ARRHENIUS PLOT FOR ELECTRODES WITH VARYING ELECTROCATALYST. 300 and 500 mV POLARIZATION



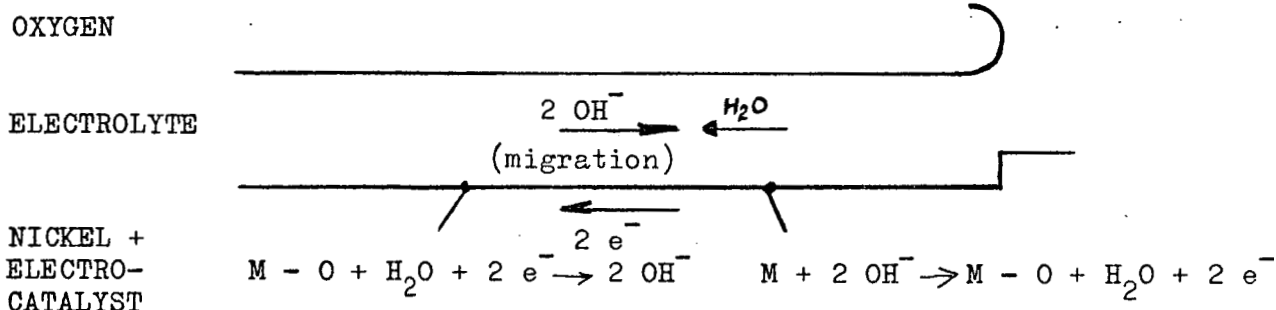
PROCESSES IN A POROUS ELECTRODE BEFORE AND AFTER CURRENT INTERRUPTION

BEFORE CURRENT INTERRUPTION:

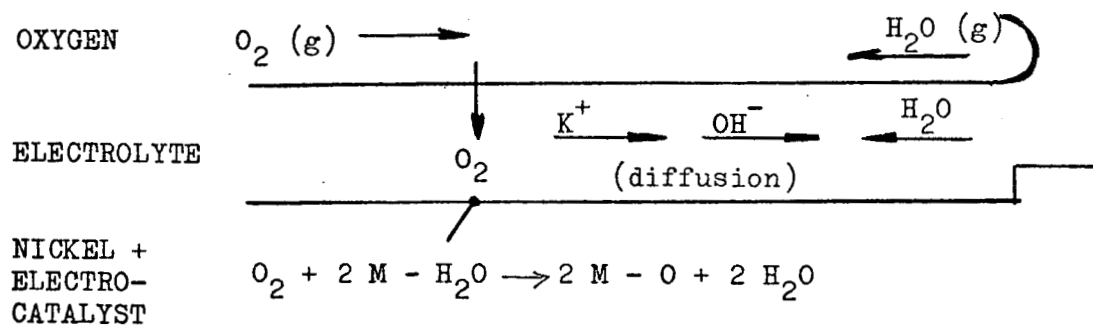


AFTER CURRENT INTERRUPTION:

SHORT CIRCUIT CURRENTS:



Diffusion and electrosorption:



Decomposition of peroxide:

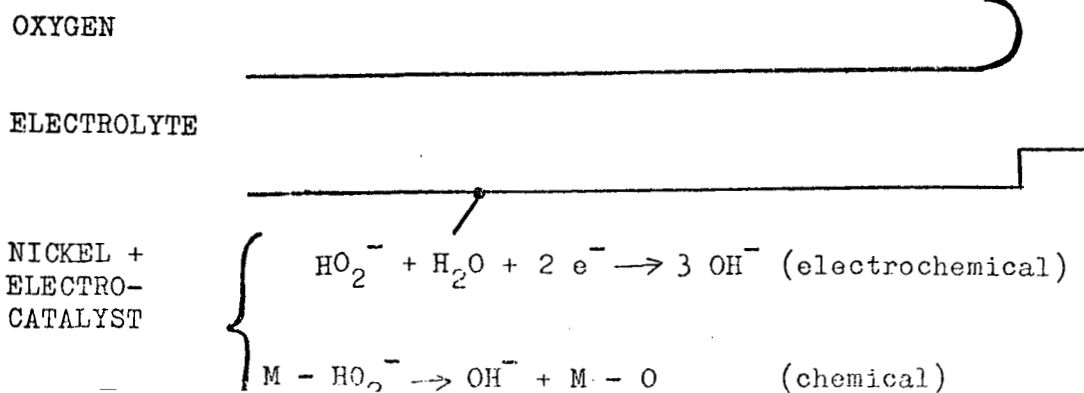
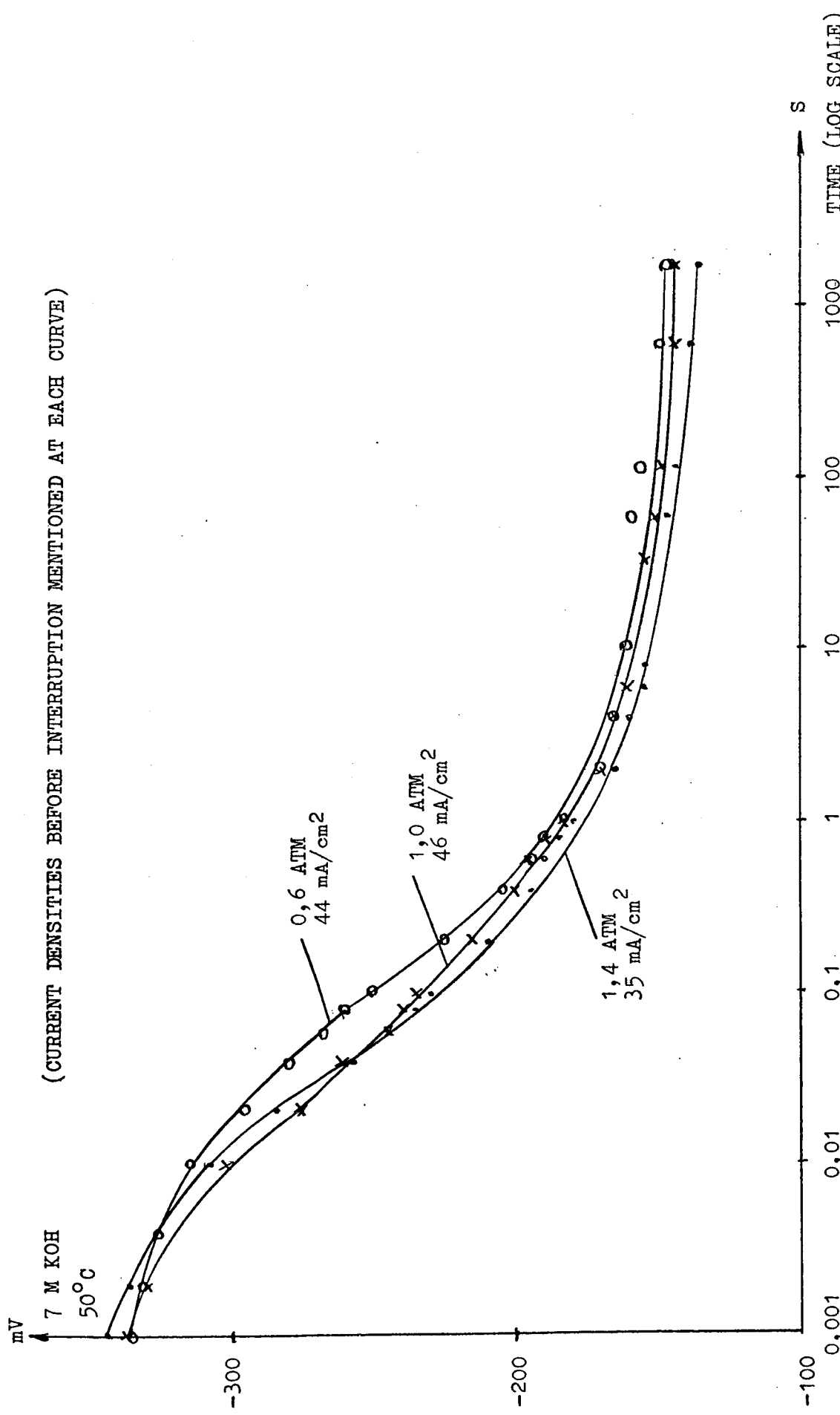


FIG 9

POLARIZATION DECAY FOR AN ELECTRODE WITH SILVER ELECTROCATALYST FROM 350 mV POLARIZATION. VARYING DIFFERENTIAL PRESSURE

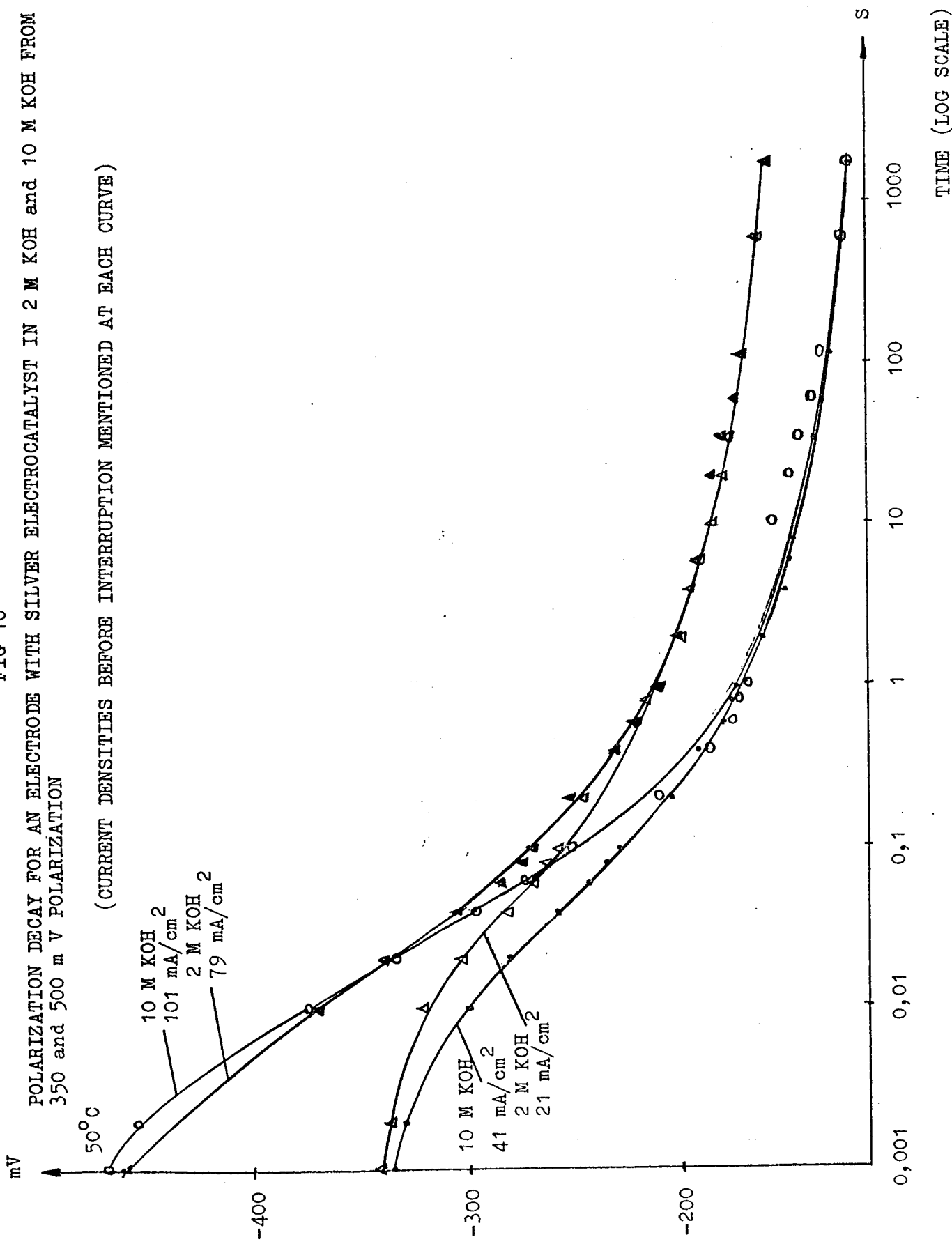
(CURRENT DENSITIES BEFORE INTERRUPTION MENTIONED AT EACH CURVE)



POTENTIAL VS REVERSIBLE OXYGEN ELECTRODE (SAME ELECTROLYTE)

FIG 10  
POLARIZATION DECAY FOR AN ELECTRODE WITH SILVER ELECTROCATALYST IN 2 M KOH AND 10 M KOH FROM 350 and 500 mV POLARIZATION

(CURRENT DENSITIES BEFORE INTERRUPTION MENTIONED AT EACH CURVE)

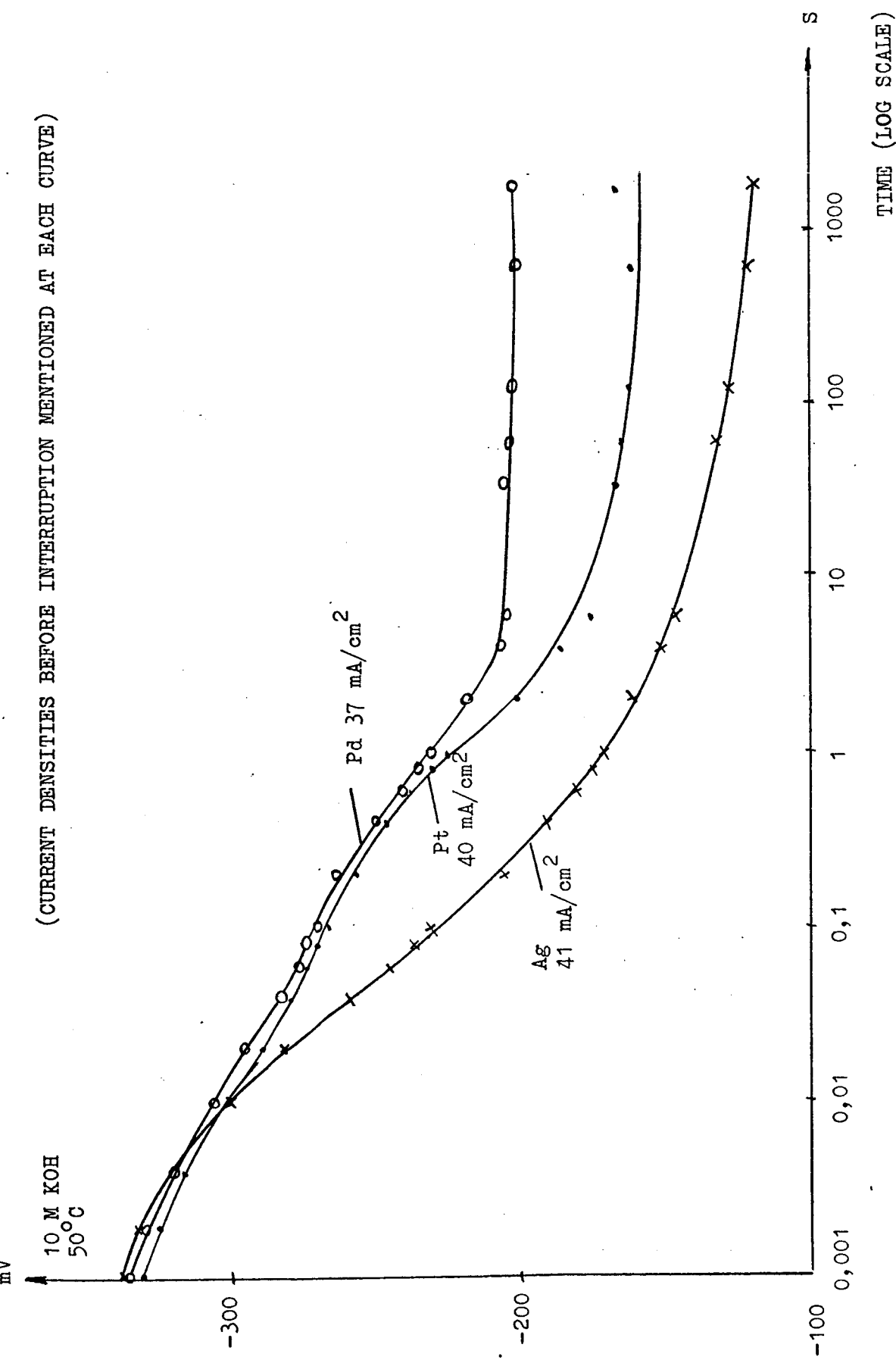


POTENTIAL VS REVERSIBLE OXYGEN ELECTRODE (SAME ELECTROLYTE)

POLARIZATION DECAY FROM 350 mV POLARIZATION. VARYING ELECTROCATALYSTS

FIG. 11

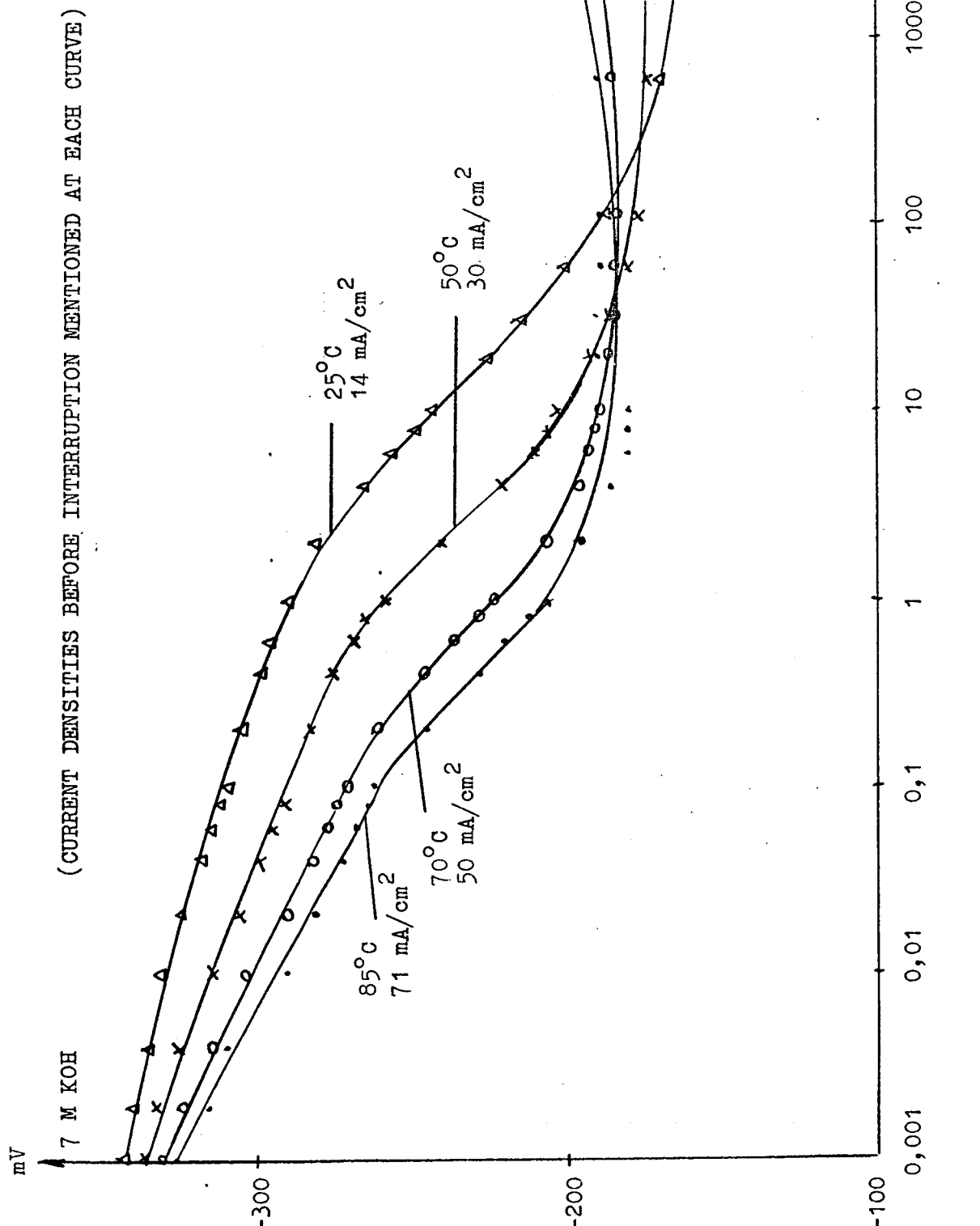
(CURRENT DENSITIES BEFORE INTERRUPTION MENTIONED AT EACH CURVE)



POTENTIAL VS REVERSIBLE OXYGEN ELECTRODE (SAME ELECTROLYTE)

FIG. 12

POLARIZATION DECAY FROM 350 mV POLARIZATION FOR AN ELECTRODE WITH PLATINUM ELECTROCATALYST.  
VARYING TEMPERATURE



POTENTIAL VS REVERSIBLE OXYGEN ELECTRODE (SAME ELECTROLYTE)

FIG 13

RELATIVE VOLUME OF SOLID, LIQUID AND GAS IN THE ACTIVE LAYER AS A FUNCTION OF DIFFERENTIAL PRESSURE

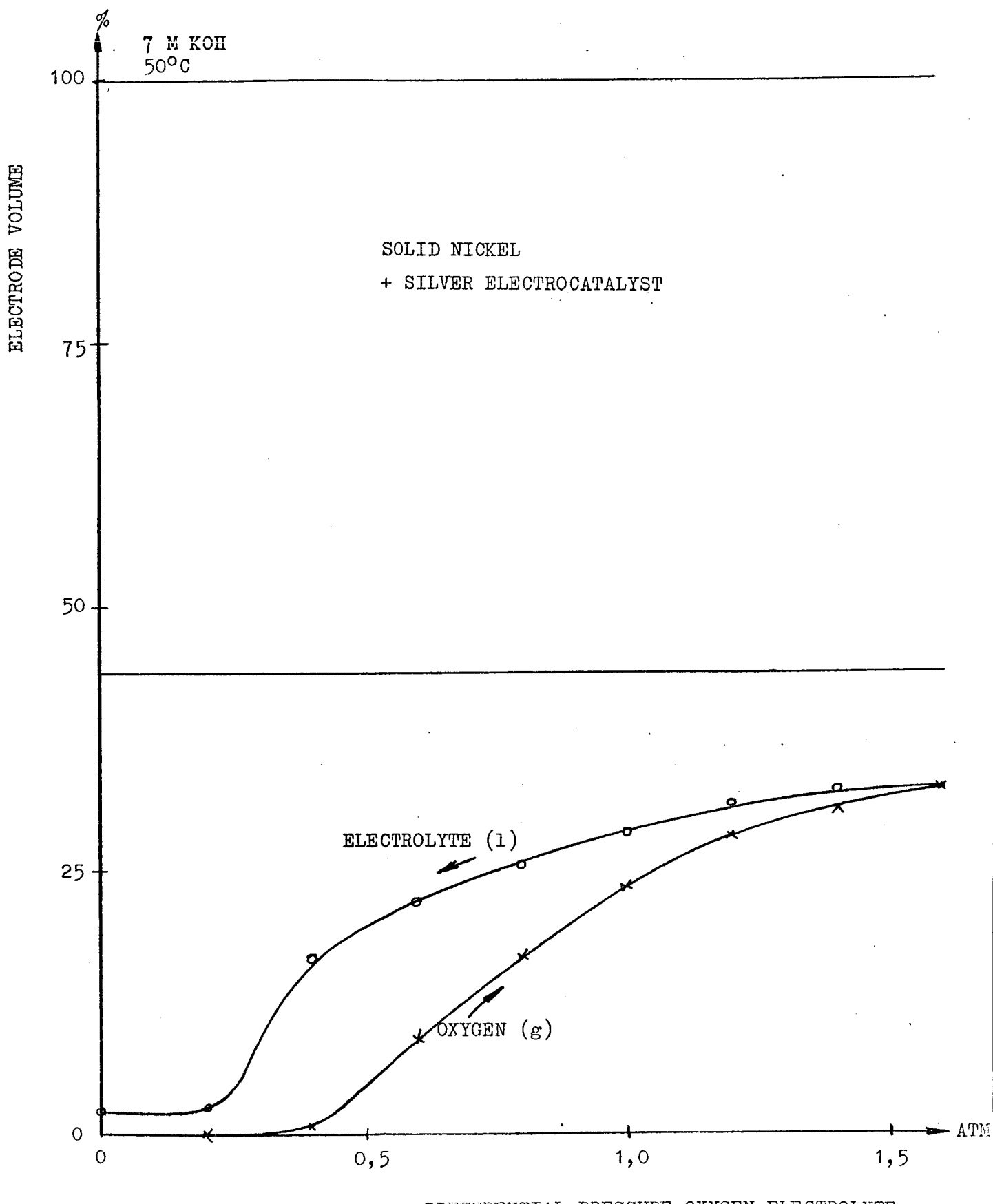


FIG 14

FILM AREA  $\text{cm}^2/\text{cm}^2$  ELECTRODE AS A FUNCTION OF DIFFERENTIAL PRESSURE

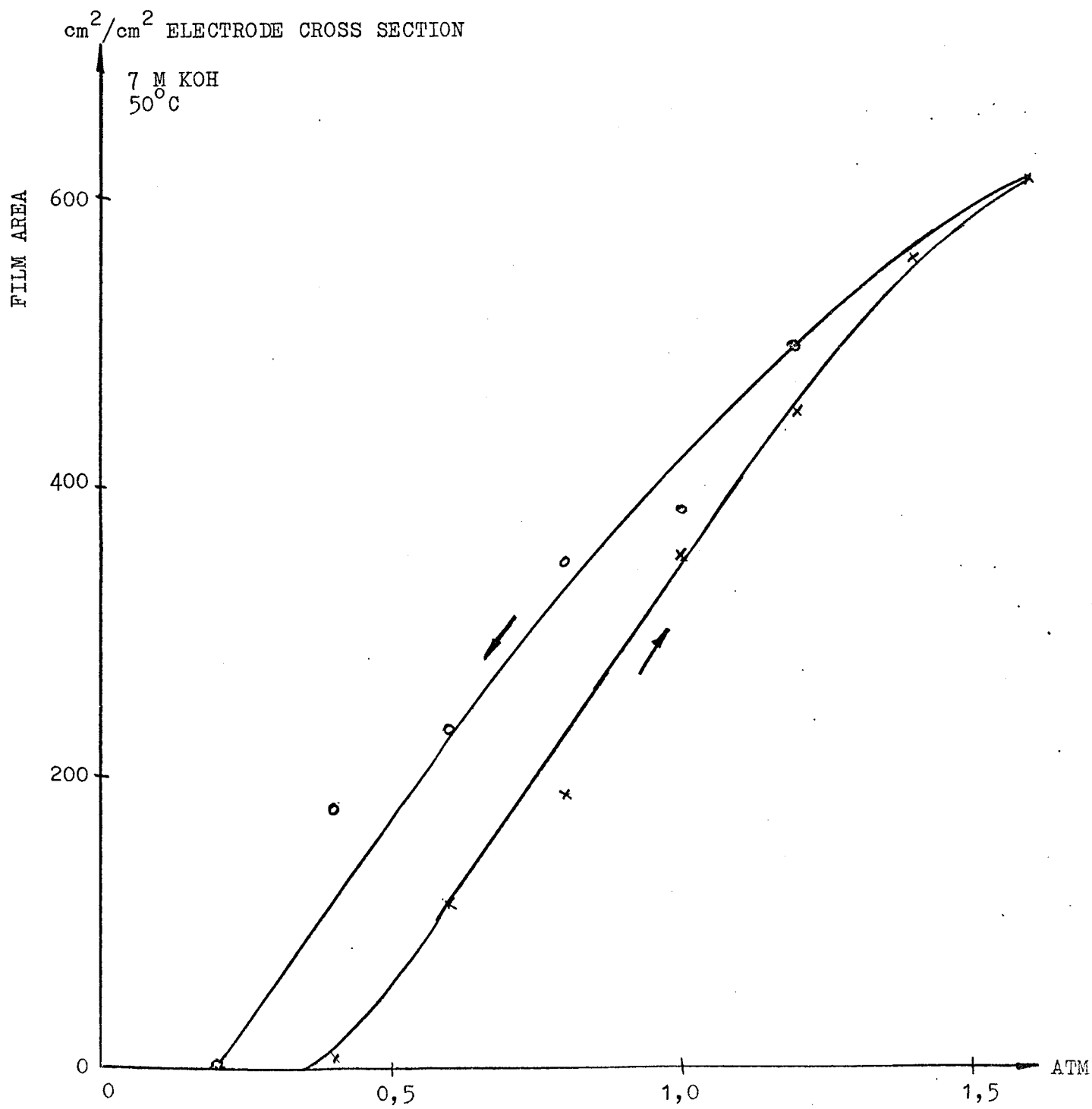


FIG 15

## FILM RESISTANCE AS A FUNCTION OF DIFFERENTIAL PRESSURE

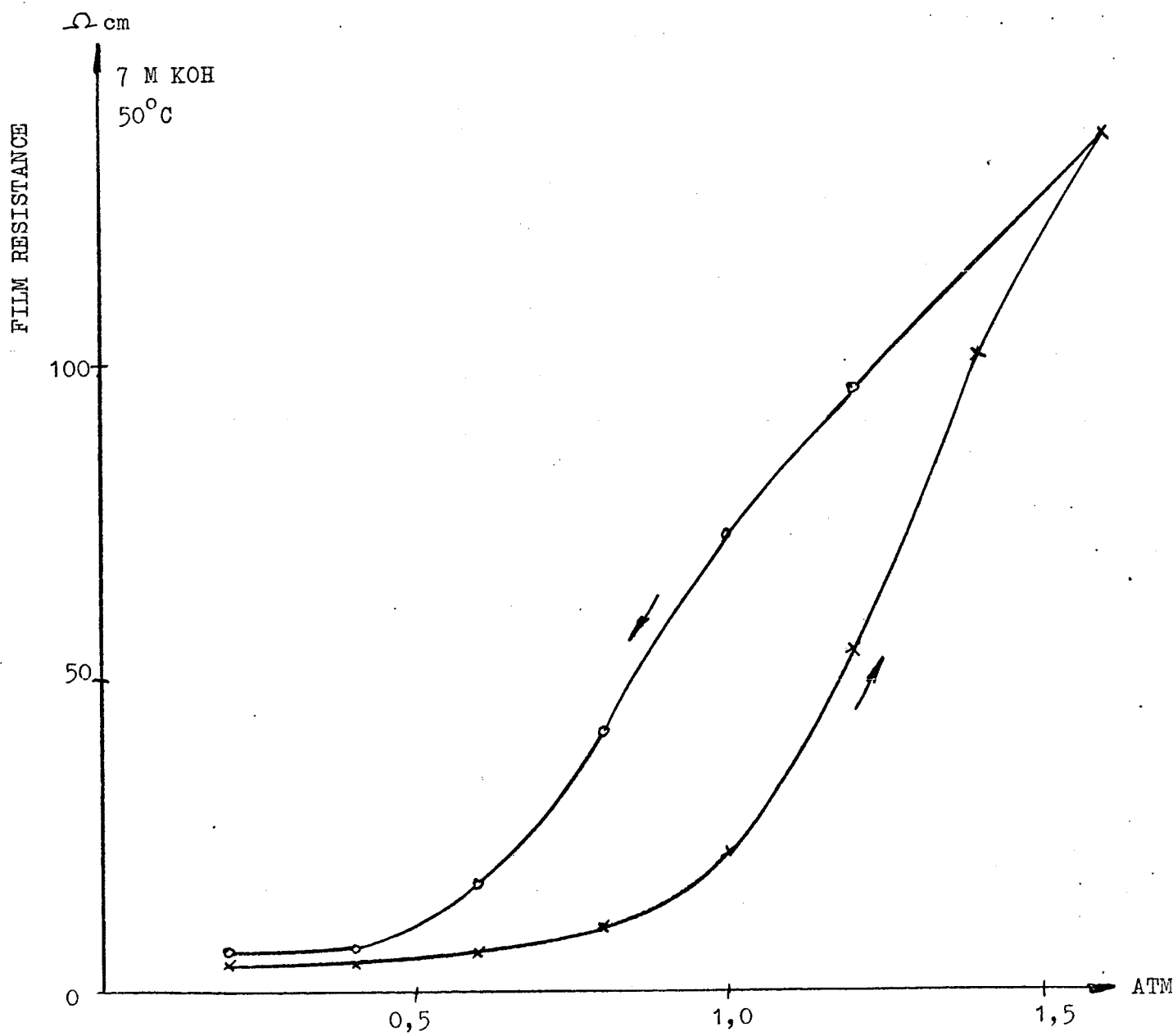


FIG 16

RELATIVE FILM CONDUCTIVITY AS A FUNCTION OF THE AMOUNT OF ELECTROLYTE  
IN THE PORE VOLUME

x = increasing differential pressure  
o = decreasing differential pressure

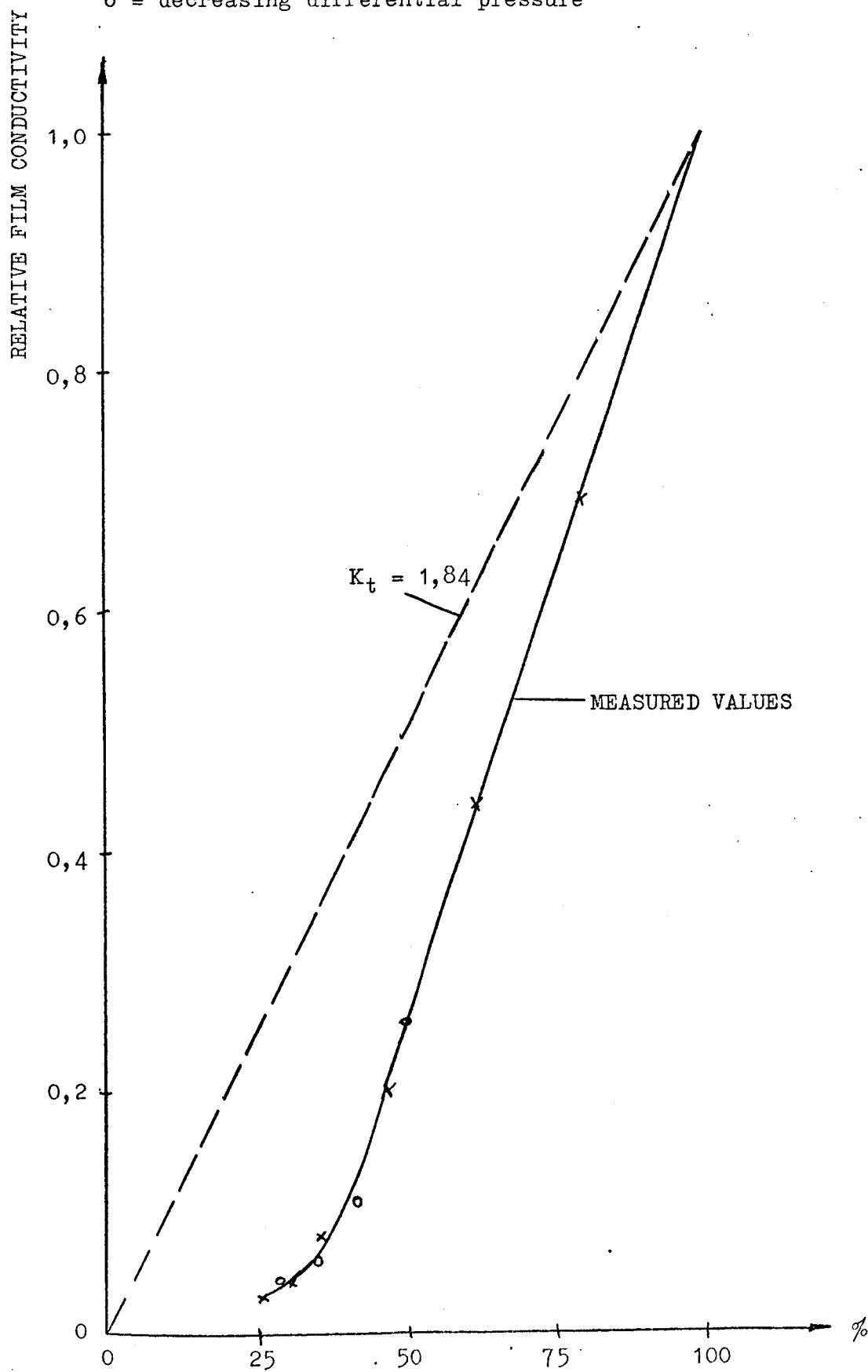
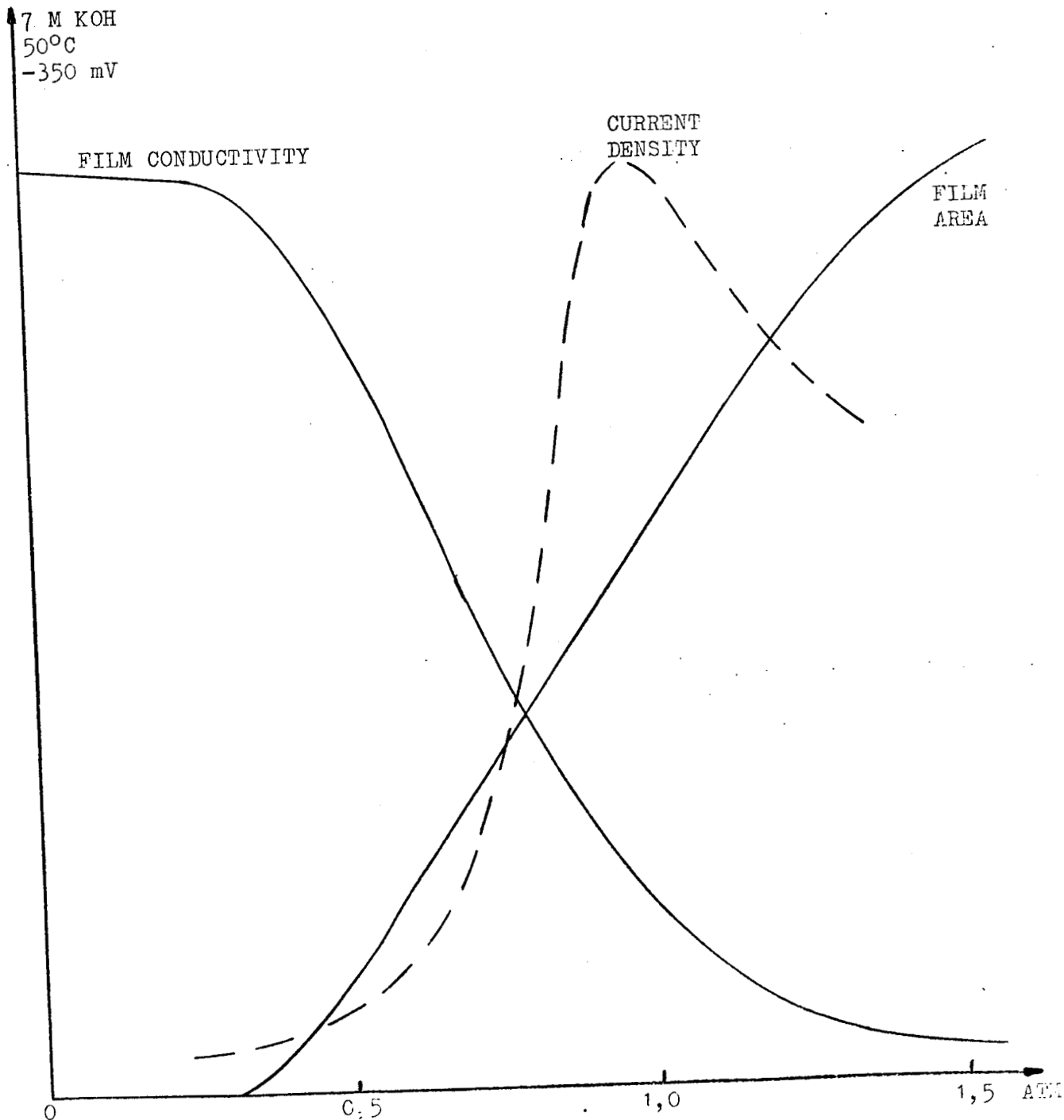


FIG. 17

FILM CONDUCTIVITY, FILM AREA AND CURRENT DENSITY AS A  
FUNCTION OF DIFFERENTIAL PRESSURE. SILVER ELECTROCATALYST. INCREASING DIFFERENTIAL PRESSURE.



DIFFERENTIAL PRESSURE OXYGEN-ELECTROLYTE

COMPARISON OF THE SHAPE OF OUR EXPERIMENTAL CURVES WITH NUMERICAL CALCULATIONS FOR THE "THIN-FILM MODEL."

FIG 18

